

Distributional data analysis via quantile functions and its application to modelling digital biomarkers of gait in Alzheimer's Disease

Rahul Ghosal^{1,*}, Vijay R. Varma², Dmitri Volfson³, Inbar Hillel⁴, Jacek Urbanek⁵,

Jeffrey M. Hausdorff^{4,6,7}, Amber Watts⁸ and Vadim Zipunnikov¹

¹ Department of Biostatistics, Johns Hopkins Bloomberg School of Public Health, Baltimore, Maryland USA

² National Institute on Aging (NIA), National Institutes of Health (NIH), Baltimore, Maryland, USA

³Neuroscience Analytics, Computational Biology, Takeda, Cambridge, MA, USA

⁴Center for the Study of Movement, Cognition and Mobility, Neurological Institute,
Tel Aviv Sourasky Medical Center, Tel Aviv, Israel

⁵ Department of Medicine, Johns Hopkins University School of Medicine, Baltimore Maryland, USA

⁶ Department of Physical Therapy, Sackler Faculty of Medicine, and Sagol School of Neuroscience,
Tel Aviv University, Tel Aviv, Israel

⁷Rush Alzheimer's Disease Center and Department of Orthopedic Surgery,
Rush University Medical Center, Chicago, USA

⁸ Department of Psychology, University of Kansas, Lawrence, KS, USA

**email*: rghosal@ncsu.edu

SUMMARY: With the advent of continuous health monitoring via wearable devices, users now generate their unique streams of continuous data such as minute-level physical activity or heart rate. Aggregating these streams into scalar summaries ignores the distributional nature of data and often leads to the loss of critical information. We propose to capture the distributional properties of wearable data via user-specific quantile functions that are further used in functional regression and multi-modal distributional modelling. In addition, we propose to encode user-specific distributional information with user-specific L-moments, robust rank-based analogs of traditional moments. Importantly, this L-moment encoding results in mutually consistent functional and distributional interpretation of the results of scalar-on-function regression. We also demonstrate how L-moments can be flexibly employed for analyzing joint and individual sources of variation in multi-modal distributional data. The proposed methods are illustrated in a study of association of accelerometry-derived digital gait biomarkers with Alzheimer's disease (AD) and in people with normal cognitive function. Our analysis shows that the proposed quantile-based representation results in a much higher predictive performance compared to simple distributional summaries and attains much stronger associations

000 0000

with clinical cognitive scales.

KEY WORDS: Wearable data; Quantile functions; L-Moments; Scalar-on-function regression; JIVE; Alzheimer's disease; Gait

1. Introduction

Wearables now generate continuous streams of data such as minute-level physical activity or heart rate. These streams are a rich source of information and can be used for deeper understanding of human behaviours and their influence on human health and disease. Common analytical practice in many epidemiological and clinical studies employing wearables is to use simple scalar, or average summaries such as total activity count (TAC), minutes of moderate-to-vigorous-intensity physical activity (MVPA) (Varma et al., 2017; Bakrania et al., 2017) or total step count (TSC) (Reider et al., 2020; Mc Ardle et al., 2020). However, collapsing the entire stream of data into a single metric completely ignore temporal and distributional nature of the data.

Temporal aspect of wearable data can be accounted for with functional data analysis (FDA) that treats wearable data streams as functional observations recorded over 24 hours (Morris et al., 2006; Xiao et al., 2015; Goldsmith et al., 2016, 2015). Associations between accelerometric functional profiles and variables of interest such as health outcomes, age, and others can be studied within FDA using scalar-on-function (SOFr) or function-on-scalar (FOSr) regression (Morris, 2015) models. In addition to diurnal (over 24-hour) modelling, FDA approaches help to model weekly and seasonal variation in accelerometric signal (Huang et al., 2019; Xiao et al., 2015). Co-registration (or warping) is often a desirable pre-processing step to make sure the amplitude and phase variations are properly separated during diurnal modelling (Dryden and Mardia, 2016; Wrobel et al., 2019).

Distributional aspect of wearable data can be captured via modelling user-specific distributions. Augustin et al. (2017) proposed to summarize accelerometry activity counts recorded over 24-hours with user-specific histograms. They proposed to use these histograms as predictors in scalar-on-function regression. The main limitations of this approach include i) possibly unequal (effective) support across user-specific histograms, ii) inability to model

specific quantiles of the distribution, which, as it will be demonstrated below, could be of a great practical interest, iii) scale-dependence.

In this article, we put forward an alternative to [Augustin et al. \(2017\)](#) and propose to use user-specific quantile functions to capture the distributional nature of wearable data. Our approach overcomes the limitations i) and ii) above and provides a more flexible way to summarize distributional properties of wearable data. There is rich literature on quantile functions ([Gilchrist, 2000](#); [Powley, 2013](#)) in statistical modelling and decision theoretic analysis. Quantile functions enjoy many mathematical properties, which make them particularly useful for distributional modelling. Quantile representations have been used in symbolic data literature for regression modelling of both quantile functions responses and predictors. The approach is based on the use of ℓ_2 Wasserstein distance ([Irpino and Verde, 2013](#); [Verde and Irpino, 2010](#)). [Zhang and Müller \(2011\)](#) proposed a method for density function estimation using a quantile synchronization approach, instead of using the cross-sectional average density which does not incorporate time-warping. Recently, ([Yang et al., 2020](#)) and ([Yang, 2020](#)) proposed quantile-function-on-scalar regression approaches for modelling quantile functions as outcomes. Having quantile functions as outcomes imposes constraints on the regression that requires a regression approximant to be a valid quantile function. In our regression applications, we do not have these constraints because user-specific quantile functions are functional predictors.

Additional motivation for the proposed quantile-function approach stems from multiple research efforts aimed at discovering digital biomarkers based on distributional properties of wearable data. Stride-velocity-q95, a 95-percentile of accelerometry-estimated stride velocity, is one of the very first digital biomarkers approved as a secondary endpoint by the European Medicines Agency (EMA), a European counterpart of the Federal Drug Administration in the US ([Haberkamp et al., 2019](#)). This measure has been demonstrated to be much more

sensitive for tracking longitudinal decline in children with Duchenne muscular dystrophy compared to the mean stride-velocity. Another example comes from accelerometry-estimated gait which is often quantified via user-specific averages, measures of variability (such as standard deviation), and asymmetry (such as skewness) of gait parameters (Hausdorff et al., 2018; Shema-Shiratzky et al., 2020) estimated over a wear-period. Thus, wearable applications actively employ various distributional or quantile based user-specific summaries.

As a motivating study, we will focus on continuous accelerometry data collected over one week in a sample of 86 community-dwelling older adults with mild Alzheimer’s disease (AD) and cognitively normal controls (CNC)(Varma and Watts, 2017; Varma et al., 2021). AD is the most common form of dementia and cases are projected to more than double in the next 40 years (Alzheimer’s Association, 2020; Hebert et al., 2013). Digital biomarkers have recently been considered for early detection of AD as an alternative to more invasive and expensive fluid and imaging markers (Kourtis et al., 2019). Specifically, digital biomarkers that reflect alterations in gait may help to predict AD due to the close relationship between complex cognitive functions and gait (Yogev-Seligmann et al., 2008; Varma et al., 2021). In our study subjects wore an accelerometer on their hip in order to measure continuous, community activity over 7 days. Using a validated processing pipeline (Weiss et al., 2014), we measured 52, domain-specific gait parameters during identified episodes of sustained walking (defined as walking longer than 60 seconds) over the course of the 7-day data collection period.

Figure 1 shows the user-specific quantile functions of accelerometry-estimated step velocity for mild-AD and CNC group.

[Figure 1 about here.]

Interestingly, for each group, the average quantile function is directly related to the Wasserstein barycenter of their respective distribution (Bigot et al., 2018). The average quantile functions, therefore, can be highly informative and can identify parts of the distribution

that are most discriminative between groups of interest. The largest difference between the two groups can be seen in the upper quantiles of step velocity. This supports the point that quantile functions can be useful for distributional representations.

Three main methodological contributions of this article are as follows. First, we propose to capture the distributional properties of wearable data via user-specific quantile functions and use them as predictors in scalar-on-function regression. This approach is further generalized using functional generalized additive model ([McLean et al., 2014](#)) which can capture possible nonlinear effects of the quantile functions. Such models have strong mathematical interpretations as linear functional of quantile functions or its transformation is known to encode several important characteristics of a continuous distribution ([Powley, 2013](#)). Second, we propose to use L-moments to represent user-specific quantile functions via functional decompositions that also preserve distributional information. L-moments introduced in [Hosking \(1990\)](#) are robust rank based analogs of traditional moments and they fully define the distribution. Quantile functions are representable via L-moments through their projections on shifted Legendre polynomials (LP) which are orthogonal on $[0, 1]$. We show that the standard scalar-on-function regression model (SOFR) using user-specific quantile function can be reduced to a generalized linear model on its L-moments, hence providing both functional and distributional interpretability of the covariate effects. Third, in our motivating application, there are multiple digital biomarkers that can be grouped into five gait domains including Amplitude, Pace, Rhythm, Symmetry, and Variability. Thus, this gives rise to a design with multi-modal distributional data. We demonstrate how L-moments can be flexibly employed in unsupervised learning for analyzing joint and individual sources of variation in multi-modal distributional data using the JIVE (Joint and Individual Variation Explained) ([Lock et al., 2013](#)) method.

The rest of this article is organized as follows. In Section 2, we present our modelling

framework, introduce the mathematical background for quantile functions, and illustrate the proposed approach of using subject-specific quantile function in additive scalar-on-function regression. In Section 3, we introduce L-moments for distributional data and show how they can be used for SOFR and JIVE. In Section 4, we demonstrate the applications of the proposed methods in the Alzheimer’s disease (AD) study. Section 5 concludes with a discussion on the main contribution and some possible extensions of this work.

2. Modelling Framework

Suppose, we have densely observed repeated measures data X_{ij} ($j = 1, \dots, J$) for subjects $i = 1, \dots, n$, where $j = 1, \dots, J$ is typically quite large (14 days or 50-60 walking bouts). For example X_{ij} can be $X_i(t_{ij})$, where X_i is observed across various time-points t_{ij} . Assume X_{ij} ($j = 1, \dots, J$) $\sim F_i(x)$, a subject-specific cumulative distribution function (cdf), where $F_i(x) = P(X_{ik} \leq x)$. Then, we can define subject-specific quantile function $Q_i(p) = \inf\{x : F_i(x) \geq p\}$. The quantile function completely characterizes the distribution of the individual observations. In this article, we restrict our attention to cases, where both $F_i(x)$ s and $Q_i(p)$ are continuous, which ensures $Q_i = F_i^{-1}$, so $F_i(Q_i(p)) = p$, $Q_i(F_i(x)) = x$. This also ensures both quantile function and cdf are strictly increasing in their respective domains (Powley, 2013). Using X_{ij} ($j = 1, \dots, J$) one can calculate $\hat{F}_i(x)$, the empirical cdf and then obtain the empirical quantile function $\hat{q}_i(p) = \hat{F}_i^{-1}(p)$ ($p \in [0, 1]$, the percentile resolution can be determined based on the amount of available data). Estimation of quantile functions can be done via a linear interpolation of order statistics (Parzen et al., 2004) and does not require a bandwidth selection as in kernel density estimation. Quantile functions have a few nice mathematical properties (Gilchrist, 2000; Powley, 2013) that make them particularly suitable for distributional modelling. For convenience, we list some of these properties below.

- A non-negative linear combination of finite number of quantile functions is a quantile function.

- For a probability distribution defined via a quantile function $Q(\cdot)$, all integer moments can be represented as $E(X^m) = \int_0^1 Q^m(p)dp$ (assuming that all moments exist).
- The differential entropy of a continuous distribution function can be calculated as $\int_0^1 \log(Q'(p))dp$.
- The quantile density function and the p -probability density function are defined as $q(p) = Q'(p)$ and $f(Q(p))$, respectively. Here, f is the density function corresponding to F .
- Tail behaviour of the distributions can be evaluated via van-Zweet index function $\frac{Q''(p)}{Q'(p)}$ (Powley, 2013; vanZwet, 1964), which is a quantile function for log concave distributions.
- The average of subject-specific quantile functions $\bar{Q}(p) = \frac{1}{n} \sum_{i=1}^n Q_i(p)$ can be mapped to the Wasserstein barycenter of the measures induced by the respective distributions (Bigot et al., 2018).
- Expansions of quantile functions via orthogonal polynomials are directly related to the components of the Shapiro–Francia Statistic (Takemura, 1983) and L-moments (Hosking, 1990) which will be discussed in greater details in Section 3.
- In $L_2 [0, 1]$, a distance between any two quantile functions can be defined via 2-Wasserstein distance W_2 or the Mallow's $d_2^2(F_1, F_2) = \int_0^1 (Q_1(p) - Q_2(p))^2 dp$.

Next section illustrates the use of quantile functions as functional objects in scalar-on-function regression models.

2.1 Supervised Learning with quantile functions via SOFR

In this section, we assume that $Y_i, i = 1, \dots, n$ is an outcome of interest that can be continuous or discrete that comes from an exponential family. We consider the following generalized scalar-on-function regression model:

$$E(Y_i|X_{i1}, X_{i2}, \dots, X_{iJ}) = \mu_i, \quad g(\mu_i) = \alpha + \mathbf{Z}_i^T \boldsymbol{\gamma} + \int_0^1 Q_i(p) \beta(p) dp. \quad (1)$$

Here g is a known link function and $Q_i(p)$ s are the subject-specific quantile function of predictor of interest X_{ij} and scalar covariates Z_i . The smooth coefficient function $\beta(p)$

represents the functional effect of the quantile function at quantile level p . As pointed out in [Reiss et al. \(2017\)](#) locations with largest $|\beta(p)|$ are the most influential to the response and of practical interest. In the special case of $\beta(p) = \beta$, model (1) reduces to a usual GLM on the mean summary ($\nu_i = \int_0^1 Q_i(p)dp$) of repeated measures data

$$g(\mu_i) = \alpha + \mathbf{Z}_i^T \boldsymbol{\gamma} + \beta \int_0^1 Q_i(p)dp = \alpha + \mathbf{Z}_i^T \boldsymbol{\gamma} + \beta \nu_i. \quad (2)$$

Several methods exist in the literature for estimation of the smooth coefficient function $\beta(p)$ ([Goldsmith et al., 2011](#); [Marx and Eilers, 1999](#)) in scalar-on-function regression model. In this article, we follow a smoothing spline estimation method. The penalized negative log likelihood criterion for estimation is given by

$$R(\alpha, \boldsymbol{\gamma}, \beta(\cdot)) = -2\log L(\alpha, \boldsymbol{\gamma}, \beta(\cdot); Y_i, \mathbf{Z}_i^T, Q_i(p)) + \lambda \int_0^1 \{\beta''(p)\}^2 dp. \quad (3)$$

The second derivative penalty on $\beta(p)$ ensures the resulting coefficient function is smooth. We model the unknown coefficient functions $\beta(p)$ using univariate basis function expansion as $\beta(p) = \sum_{k=1}^K \beta_k \theta_k(p) = \boldsymbol{\theta}(p)^T \boldsymbol{\beta}$, where $\boldsymbol{\theta}(p) = [\theta_1(p), \theta_2(p), \dots, \theta_K(p)]^T$ and $\boldsymbol{\beta} = (\beta_1, \beta_2, \dots, \beta_K)^T$ is the vector of unknown coefficients. In this article, we use cubic B-spline basis functions, however, other basis functions can be used as well. The linear functional effect then becomes $\int_0^1 Q_i(p) \beta(p) dp = \sum_{k=1}^K \beta_k \int_0^1 Q_i(p) \theta_k(p) dp = \sum_{k=1}^K \beta_k Q_{ik} = \mathbf{Q}_i^T \boldsymbol{\beta}$. The minimization criterion in (3) now can be reformulated as,

$$R(\psi) = R(\alpha, \boldsymbol{\gamma}, \boldsymbol{\beta}) = -2\log L(\alpha, \boldsymbol{\gamma}, \boldsymbol{\beta}; Y_i, \mathbf{Z}_i, \mathbf{Q}_i) + \lambda \boldsymbol{\beta}^T \mathbb{P} \boldsymbol{\beta}, \quad (4)$$

where \mathbb{P} is the penalty matrix given by $\mathbb{P} = \{\int_0^1 \boldsymbol{\theta}''(p) \boldsymbol{\theta}''(p)^T dp\}$. This minimization can be carried out using the Newton-Raphson algorithm implemented under generalized additive models (GAM) ([Wood et al., 2016](#); [Wood, 2017](#)). The smoothing parameter λ can be chosen using REML, information criterion like AIC, BIC, or data driven methods such as Generalized CV. We use the `refund` package ([Goldsmith et al., 2018](#)) in R ([R Core Team, 2018](#)) for implementation of SOFR.

2.2 Extension of Quantile function based SOFR to FGAM

The traditional scalar-on-function regression (SOFR) model (1) assumes a linear association between the quantile function and the outcome. We extend the quantile function based SOFR model to functional generalized additive model (FGAM) of McLean et al. (2014) which can be used to capture nonlinear effects of quantile function $Q(p)$. Specifically, we model the link function $g(\cdot)$ as $g(\mu_i) = \alpha + \mathbf{Z}_i^T \boldsymbol{\gamma} + \int_0^1 F(Q_i(p), p) dp$. The bivariate function $F\{Q(p), p\}$ is smooth function on $\mathbb{R} \times [0, 1]$, capturing effect of subject-specific quantile function $Q(p)$ at quantile level p . In a special case of $F\{Q(p), p\} = Q(p)\beta(p)$, FGAM reduces to model (1). The estimation procedure for FGAM is discussed in Web Appendix 1.

Remark 1:

It can be shown that SOFR model using quantile functions of a predictor is invariant under continuous monotone transformation of predictors using equivariance property of the quantile function. The FGAM approach using quantile function is more flexible and remains invariant under any continuous transformation of predictors. (McLean et al., 2014).

3. L-moments and modelling quantile functions

L-moments were defined by (Hosking, 1990) as the expectation of a linear combination of order statistics. In particular, the r -th order L-moment of a random variable X is defined as

$$L_r = r^{-1} \sum_{k=0}^{r-1} (-1)^k \binom{r-1}{k} E(X_{r-k:r}) \quad r = 1, 2, \dots, \quad (5)$$

where $X_{1:n} \leq X_{2:n} \leq \dots \leq X_{n:n}$ denote order statistics of a random sample of size n drawn from the distribution of X . The first order L-moment equals the traditional mean. The second order L-moment is equal to the Gini's mean difference statistic divided by 2. Thus, L_2 can be seen as a robust measure of scale. Higher order L-moments are related to robust distributional summaries that can be interpreted similarly to traditional higher-order moments such as skewness and kurtosis.

In our approach, we leverage an alternative representation of L-moments as projections of

quantile functions on Legendre polynomial basis. Specifically, L-moments of order r can be represented as

$$L_r = \int_0^1 Q(p) P_{r-1}(p) dp, \quad (6)$$

where $P_r(p)$ is the shifted Legendre polynomials (LP) of degree r defined as follows

$$P_r(p) = \sum_{k=0}^r s_{r,k} p^k, \quad s_{r,k} = (-1)^{r-k} \binom{r}{k} \binom{r+k}{k} = \frac{(-1)^{r-k} (r+k)!}{(k!)^2 (r-k)!}. \quad (7)$$

Legendre polynomials have standard orthogonality properties on $[0, 1]$ as

$$\int_0^1 P_s(p) P_r(p) dp = \delta_{rs} * (1/2r + 1), \quad (8)$$

where $\delta_{rs} = I(r = s)$. The quantile function $Q(p)$ hence have this following decomposition

$$Q_k(p) = \sum_{r=1}^k (2r-1) P_r(p) \int_0^1 Q(p) P_{r-1}(p) dp = \sum_{r=1}^k (2r-1) L_r P_{r-1}(p) \rightarrow Q(p), k \rightarrow \infty, . \quad (9)$$

Note that this approximation can be poor in the tails, if the distribution is heavy tailed ([Hosking, 1990](#)). For a non negative random variable X , regular moments can be expressed as $\mu_k = EX^k = \mu_k(\bar{F}) = k \int_0^\infty x^{k-1} \bar{F}(x) dx = \mu_k(Q) = \int_0^1 Q^k(p) dp$, where $\bar{F}(x) = 1 - F(x)$, and $F(x)$ is the cumulative distribution function for X . The main advantages of L-moments over traditional moments are the following. First, all L-moments exist as long as $E(X) < \infty$. Trimmed L-moments ([Elamir and Seheult, 2003](#)) can be used, if $E(X^s) < \infty$, for some $s \in (0, 1)$. Second, L-moments are unique and fully define the distribution. Third, L-moments are defined via linear combinations of order statistics, and are typically more robust compared to the traditional moments.

A geometrical intuition behind existence of L-moments is illustrated in [Figure 2](#) that shows a comparison between $\mu_k(\bar{F})$, $\mu_k(Q)$ and $L_k(Q) = \int_0^1 Q(p) P_{k-1}(p) dp$ for a log-normal and a Beta distribution.

[Figure 2 about here.]

Note that the integrals for $\mu_k(\bar{F})$, $kx^{k-1}\bar{F}(x)$ can diverge over x . Similarly, the integrals for

$\mu_k(Q)$, $Q^k(p)$ can diverge over p . However, functions $Q(p)P_{k-1}(p)$ always lie between $Q(p)$ and $-Q(p)$, which guarantees the existence of all moments as long as $\int_0^1 Q(p)dp < \infty$.

3.1 Scalar-on-function regression (SOFR) using L-moments

In this section, we develop a scalar-on-function regression method using subject-specific L-moments. This approach will allow us to simultaneously interpret the results of SOFR both in terms of functional effects of quantile functions as well as in terms of the effects of specific L-moments.

The representation of the quantile function in (9) allows us to define an inner product between two quantile functions for subjects i and j in terms of their L-moments as $\langle Q_i, Q_j \rangle = \sum_{r=1}^{\infty} (2r-1)L_{ir}L_{jr}$. Since shifted Legendre polynomials form an orthogonal basis of $L_2[0,1]$, we can expand $\beta(p)$ in model (1) as $\beta(p) = \sum_{k=1}^K \beta_k P_{k-1}(p)$. Thus, the scalar-on-function regression model (1) reduces to a standard GLM on the subject-specific L-moments as

$$g(\mu_i) = \alpha + \mathbf{Z}_i^T \boldsymbol{\gamma} + \sum_{k=1}^K \beta_k \int_0^1 Q_i(p) P_{k-1}(p) dp = \alpha + \mathbf{Z}_i^T \boldsymbol{\gamma} + \sum_{k=1}^K \beta_k L_{ik}. \quad (10)$$

Unknown basis coefficients β_k in this representation capture a linear effect of the L-moments of the subject-specific distribution. Note that the first order L-moment L_1 equals mean of the subject-specific distribution, therefore, model (10) is more general than using the subject-specific mean.

This approach can be seen as somewhat analogous to functional principal component regression (fPCR) method (Reiss et al., 2017), where fPC scores are used for supervised learning. L-moments are projections on orthogonal basis functions and, hence, can be interpreted in similar additive manner while additionally providing moment-based characterization of underlying distributions. The number of L-moments K to be retained can be treated as a tuning parameter and can be chosen in a data driven way using cross-validation or

information criteria such as AIC or BIC. It is important to note that the proposed approach allows mutually consistent interpretation of the results from the quantile-level perspective via $\beta(p)$ and from the distributional L-moment level perspective via β_k 's.

Nonlinear associations can be modelled using nonlinear scalar-on-function regression (Reiss et al., 2017) that can be seen as a functional analogue of single index model (Stoker, 1986). In particular, the model is given by

$$E(Y_i|X_{i1}, X_{i2}, \dots, X_{iJ}) = \mu_i, \quad g(\mu_i) = \alpha + \mathbf{Z}_i^T \boldsymbol{\gamma} + h\left(\int_0^1 Q_i(p)\beta(p)dp\right), \quad (11)$$

where $h(\cdot)$ is a smooth unknown function on real line. Expanding $\beta(p)$ via Legendre polynomial basis, we get a traditional single index model where the L-moments play a role of predictors as $g(\mu_i) = \alpha + \mathbf{Z}_i^T \boldsymbol{\gamma} + h(\mathbf{L}_i^T \boldsymbol{\beta})$. Traditional estimation methods for single index model (Wang and Yang, 2009; Ichimura, 1991) can be applied to estimate both $h(\cdot)$ and $\boldsymbol{\beta}$.

An alternative way to capture nonlinear association between the outcome and quantile functional predictors is to use a generalized additive model (GAM) with L-moments as $g(\mu_i) = \alpha + \mathbf{Z}_i^T \boldsymbol{\gamma} + \sum_{k=1}^K h_k(L_{ik})$. The GAM approach using L-moments is analogous to the “functional additive model” of Müller and Yao (2008), where fPC scores were used for scalar-on-function modelling and offers additional interpretability in terms of nonlinear effects of robust distributional summaries of data.

3.2 Joint and Individual Variation Explained for multimodal distributional data via

L-moments

In this section, we demonstrate how L-moments can be used to identify joint and individual sources of variation in multi-modal distributional data. Suppose, we have repeated measures data from multiple domains $d = 1, 2, \dots, D$ each consisting of K_d different features on the same subjects $i = 1, 2, \dots, n$. Thus, we have subject-specific quantile functions $Q_i^{(d, r_d)}(p)$ for r_d -th feature within domain d ($r_d = 1, 2, \dots, R_d$). In many applications, it is important

to identify joint and individual sources of variation in these multi-modal distributional data. For scalar data, [Lock et al. \(2013\)](#) introduced joint and individual variation explained (JIVE) for integrative analysis of data coming from multiple domains. JIVE decomposes the original block data matrix into three parts, a low rank approximation capturing the joint structure and low rank approximations capturing domain-specific individual variation and noise. For multi-modal distributional data $Q_i^{(d,r_d)}(p)$, we propose to use L-moments for analyzing joint and individual sources of variation. This enables us to decompose the distributional variation captured via L-moments into joint and individual sources. Specifically, let $L_{ik}^{(d,r_d)} = \int_0^1 Q_i^{(d,r_d)}(p)P_{k-1}(p)$ be the k -th L-moment ($k = 1, 2, \dots, K$) for $Q_i^{(d,r_d)}$. For each feature, we form the vector of L-moments and denoting it as $\mathbf{L}_i^{(d,r_d)}$. Then, for each domain d , we get the following vector of L-moments $\mathbf{L}_i^{(d)} = [\mathbf{L}_i^{(d,1)^T}, \mathbf{L}_i^{(d,2)^T}, \dots, \mathbf{L}_i^{(d,R_d)^T}]^T$, where $\mathbf{L}_i^{(d)}$ is a $v_d = KR_d$ -dimensional vector consisting of all L-moments for all features in domain d . Next, we apply JIVE decomposition of these L-moments vectors as $\mathbf{L}_i^{(d)} = \mathbf{J}_i^d + \mathbf{A}_i^d + \boldsymbol{\varepsilon}_i^d = \Phi_J^d \boldsymbol{\xi}_{J,i} + \Phi_A^d \boldsymbol{\xi}_{A,i}^d + \boldsymbol{\varepsilon}_i^d$. Here, \mathbf{J}_i^d and \mathbf{A}_i^d represent the low rank joint and individual structures with rank s and s_d , respectively, and $\boldsymbol{\varepsilon}_i^d$ is the residual noise. Matrices of loadings for joint and individual structures are given by $\Phi_J^d \in \mathbb{R}^{v_d \times S}$, $\Phi_A^d \in \mathbb{R}^{v_d \times S_d}$, and $\boldsymbol{\xi}_{J,i}$, $\boldsymbol{\xi}_{A,i}^d$ are corresponding joint and individual scores for subject i . The summary of the proposed JIVE approach is presented as an Algorithm in Web Appendix 2. The ranks s , s_d can be chosen using BIC or permutation tests ([Lock et al., 2013](#)). The number of L-moments K can be chosen beforehand in a data-driven way. The joint and individual scores $\boldsymbol{\xi}_{J,i}$, $\boldsymbol{\xi}_{A,i}^d$ can further be used for supervised learning purposes. We use the `r.jive` package ([O'Connell and Lock, 2017](#)) in R ([R Core Team, 2018](#)) for implementation of JIVE.

4. Digital gait biomarkers in Alzheimers' Disease

Data for this study ([Varma et al., 2021](#)) were collected using a GT3x+ tri-axial accelerometer in a sample of older adults including mild-AD ($n = 38$) and age-matched cognitively normal

controls (CNC) ($n = 48$). The accelerometer was placed on the dominant hip of the participants via elastic belt. Activity was monitored continuously for seven days and, subsequently, gait parameters were obtained using a processing pipeline developed and validated in the Parkinson’s Disease (PD) field (Weiss et al., 2014). The pipeline outputs 52 gait metrics coming from 5 gait domains of Amplitude (8 metrics), Pace (3 metrics), Rhythm (13 metrics), Symmetry (9 metrics), and Variability (19 metrics). The complete list of gait metrics, along with their description and associated domains have been described in Varma et al. (2021) and is given in Web Table 4. Each gait metric is calculated every time a subject completes a sustained bout of walking of at least 60 sec; this provides multiple observations per subject across each of the seven wear days. Figure 1 reveals distributional nature of this data for a particular gait metric “step velocity” for AD and CNC group.

Along with the gait metrics, we also have data on several baseline variables e.g., age, sex, BMI, years of education, V_{O_2} max (maximum rate of oxygen consumption during a treadmill test) on each subject. Descriptive statistics of these variables for the complete, AD, and CNC samples are displayed in Web Table 1. We will start with SOFR and FGAM approaches using quantile functions of the digital gait biomarkers to model mild-AD status (Varma et al., 2021). Subsequently, we illustrate SOFR via L-moment representation of quantile functions to study associations between digital gait biomarkers and cognitive functioning. Finally, we will perform JIVE on multi-modal digital gait biomarkers to identify their joint and individual sources of variation and then associate them with cognitive functioning.

4.1 Discrimination of AD using Gait Biomarkers

One of the primary objectives of the AD study was to explore how well digital gait biomarkers can discriminate between mild-AD and CNC. To do that, we perform SOFR and FGAM with logit-link to model mild-AD vs CNC. We fit multiple models using each gait metrics separately and adjust for age and sex. For evaluation of the models, we use the “deviance

explained” criterion in GAM (Wood, 2017), which represents the proportion of null deviance explained by the respective models. Table 1 displays the top ten gait metrics ranked according to deviance explained in SOFR and FGAM.

[Table 1 about here.]

The variables in FGAM consistently explain higher deviance which is expected. Particularly interesting are “Mean_Stride_Time_s_” (mean stride time) and “Mean_Step_Time_s_” (mean step time). Used within FGAM, they explain a much higher proportion of deviance (0.63) compared to SOFR (0.37). This might be due to possible nonlinear effects of the quantile functions for these variables. The metrics “Step_Velocity_cm_sec_” (step velocity), “Distance_m_” (distance), “Cadence_V_time_domain_” (cadence) perform more or less similarly using either SOFR or FGAM, indicating a linear effect. Figure 3 displays the estimated functional effects for the top 2 metrics for SOFR, “strRegAP” (stride regularity) and step velocity, along with their average quantile functions. We see a clear negative effect in the upper quantiles for both step velocity and stride regularity, indicating higher the maximal performance for these measures lower the odds of AD, which is very interesting from a clinical perspective.

[Figure 3 about here.]

The additive quantile functional effects of the metrics mean stride time and step velocity obtained using FGAM are displayed in Web Figure 1 along with the average quantile functions of AD and CNC groups. The sliced effect of the corresponding surfaces are shown in Web Figure 2. For mean stride time, both tails can be informative. Interestingly, a higher maximal or minimal performance of this metric seems to be associated with higher odds of AD. There is a visible non-linearity in the upper tail of the estimated bivariate surface and the sliced effect $\hat{F}(q, p)$. FGAM captures this non-linearity and therefore produces a superior performance for this metric in terms of deviance explained (63%) compared to the SOFR

model (37%). The estimated bivariate surface of the quantile effect is more or less linear in quantile level (q) for step velocity and is highly negative in the upper tail (evident from the sliced effect). Hence high maximal performance in this metric is associated with lower odds of AD. Since the effect of the quantile function for this metric is linear, the performance and inference from FGAM are similar to what we obtain from SOFR.

4.2 *SOFR via L-moments*

In this section, we illustrate the application of L-moments in SOFR. In particular, we use stride regularity, step velocity, and cadence (among the top-performing metrics in SOFR) and derive the first 4 L-moments of these metrics for each subject. Compared to traditional or central moments, L-moments are orthogonal projections on the shifted Legendre polynomials. As an illustration, we display the heatmap of sample correlation among the first four L-moments, traditional and central moments of the gait metric cadence in Web Figure 3. As can be noticed the traditional and central moments are highly correlated among themselves, unlike the L-moments.

Next, we fit three separate logistic regression models for each of the gait metrics using their L-moments to model mild-AD status. The results are reported in Table 2.

[Table 2 about here.]

Importantly, it is not the mean (equal to the first order L-moment), but the second (L_2) or third-order L-moments (L_3) which have a significant effect on odds of AD for all the three gait metrics. Considering predictive performance, model A2 with step velocity is found to be the best among the three models considered, in terms of the highest proportion deviance explained (48.75%). Stride regularity explains a much lower proportion of deviance (21.58%) compared to SOFR using quantile function (58%), which indicates there might be higher order L-moments for stride regularity which are important to consider. Upon further exploration using the first 8 L-moments of stride regularity, we do find the L-moments of

orders 5, 6 and 8 to be significant and this also improves the model performance (deviance explained=55.81% using L_2, L_5, L_6, L_8). We display the resulting coefficient functions from SOFR with L-moments in Web Figure 4. The coefficient functions $\beta(p)$ obtained with traditional SOFR and SOFR with L-moments are very similar, but the latter approach provides additional L-moments interpretability.

For comparison, we provide results from a similar analysis using the first four traditional and central moments in Web Table 2 and 3, respectively. The effect of the gait measures are much weaker and not significant (at nominal level $\alpha = 0.05$) for traditional moments, possibly due to high correlation among themselves. Central moments perform similarly to L-moments. However, they do not provide a simple way to additionally interpret quantile level effects as can be done in SOFR with L-moments.

In addition to the cognitive status, this study used confirmatory factor analysis (CFA) to derive cognitive scores for attention (ATTN), verbal memory (VM) and executive function (EF), which represent a continuous scale of cognitive functioning. We study association of the L-moments of stride regularity, step velocity and cadence with the cognitive scores of ATTN, VM and EF using a linear regression model, while adjusting for age, sex and education. The results are displayed in Table 3.

[Table 3 about here.]

We observe the cognitive scores of ATTN, VM and EF to be associated with sex, education and primarily the second (L_2) order L-moments. For all the measures considered, this association is found to be positive, indicating higher L_2 moments are associated with higher cognitive scores and lower odds of dementia, which matches with our earlier analysis. The signal for the cognitive scores of VM and EF are found be much stronger (adjusted R-squared 35% – 40%) compared to ATTN (adjusted R-squared 19% – 24%). All three gait measures provide more or less similar predictive performance and significant gains compared

to a benchmark model on age, sex and education and competing models on mean of the gait metrics (around 30% – 40% improvement) in terms of adjusted R-squared criterion. Results from GAM using the L-moments of the gait measures discussed in Section 4.2 are reported in Web Table 5. The effect of the second order L-moment is again found to be most significant for the gait measures in all the models considered.

Our analysis using L-moments demonstrates there is a significant association between the gait metrics and cognitive function, illustrates that robust higher order distributional summaries of the gait measures might be more informative and hence more important to consider rather than using a single summary metric like mean (first order L moment).

4.3 JIVE with L-moments

So far in our analysis, we have considered each gait measure separately while performing SOFR with quantile functions or L-moments to study their association with cognitive performance. However, gait measures are correlated among themselves and conceptually can be placed within one of the five unique gait domains mentioned earlier. The inter-dependence of the metrics within and between the domains can be beneficial in statistical modelling and can be analyzed using JIVE approach with L-moments illustrated in Section 3.2. We focus on domains of Pace (3 features), Rhythm (13 features) and Variability (19 features) as the top performing gait metrics in the SOFR analysis (see Table 1) belong to either of these three domains. Figure 4 displays a Venn diagram illustrating a conceptual overlap of joint and individual variation across the three domains.

[Figure 4 about here.]

First, we pre-normalize variable via z-score transformation $z_i = \Phi^{-1}(F_n(x_i))$, where x_i s are the original features (subject-specific L-moments in our case). Further, all the data blocks are again normalized (centered and scaled) so that data blocks from different domains are comparable as suggested by Lock et al. (2013). Applying JIVE (O’Connell and Lock, 2017)

and determining the optimal ranks via the permutation test, we get the following ranks: (Joint, Pace, Rhythm, Variability) = (2, 2, 7, 9). Figure 5 displays the amount of variation explained by joint and individual components in each of the three domains.

[Figure 5 about here.]

Note that JIVE results in significant dimension reduction - reducing the dimension from 140 (4 L-moments from each of 35 gait metrics) to just 20. JIVE estimates of the joint and individual structures are shown in Web Figure 5.

We use JIVE scores, orthogonal by construction, to study the association with cognitive status (mild-AD). Since, we only have a relatively small sample ($n = 86$), we further perform variable selection and identify the important JIVE scores using LASSO (Tibshirani, 1996). The selected scores are joint-PC1, joint-PC2, Pace-PC1, Pace-PC2, Rhythm-PC1, Rhythm-PC2, Rhythm-PC5, Rhythm-PC7, Variability-PC4, Variability-PC7 and Variability-PC9. The results of logistic regression for cognitive status are reported in Web Table 6. To further understand the associations of JIVE PC scores with cognitive function relate them back to the original gait metrics, we use the cross-correlation between the original L-moments and the significant JIVE scores. The top 10 gait metrics (L-moments) ranked according to their correlation with each score are displayed in Figure 6.

[Figure 6 about here.]

Joint-PC1, joint-PC2 are found to be positively associated with higher odds of AD. For joint PC-1, the first order L-moments (L_1) from Pace (step velocity, distance) and Rhythm (stride regularity) are negatively loaded, indicating higher mean value for these variables e.g., step velocity lowers the odds of AD. Similarly, for joint PC-2, the second order L-moments (L_2) from Pace (step velocity, distance, mean step length) and Rhythm (cadence) are negatively loaded, indicating higher second order L-moments (representing scale) for these variables are associated with a lower risk of AD which matches with our analysis in

Section 4.2. The association between cognitive status and Rhythm-PC2, Rhythm-PC5 are found to be negative, whereas Rhythm-PC7 is found to be positively associated. Primarily, higher order L-moments (L_2, L_3, L_4) gait metrics from Rhythm and Variability are loaded on these individual PCs outlining the importance of these domains.

Our analysis in this section, using JIVE with L-moments of the gait measures provides a comprehensive summary of the joint and individual sources of variation of the gait metrics, helps in dimension reduction of the original problem, and provides better understanding of the underlying association between the gait measures and cognitive functions.

5. Discussion

Distributional data analysis is an emerging area of research that has a large number of diverse applications. There are many ways to represent distributional information including cumulative distribution function, density function, quantile function, and others. Although, all these distributional representations can be re-expressed through each other via differential, integral, inverse, or other more involved transformation, a specific choice for statistical modelling may depend on desirable interpretation and require different analytical machinery. We have proposed to capture distributional nature of data via subject-specific quantile functions and use them or their L-moment representations in SOFR, FGAM, and JIVE methods. As we argue, our approach provide many advantages including intuitive interpretation of results and uniform support on $[0, 1]$.

We have demonstrated how proposed approaches provide deeper understanding of the associations between digital gait biomarkers and cognitive functioning in Alzheimer’s disease. Specifically, we showed that quantile functions of gait metrics including step velocity, distance, cadence, stride regularity, mean stride time and mean step time provide higher discrimination between mild-AD and non-AD disease status. We also found that second order L-moments capturing subject-specific variability of a few gait parameters are significantly

associated with cognitive domains of attention, verbal memory, and executive function. JIVE analysis via L-moment representation of multi-modal distributions of gait measures revealed both joint and individual sources of variation in the domains of Pace, Rhythm and Variability.

These are many more areas that remain to be explored based on the current work. For example, it would of interest to conceptualize and accommodate distribution-level interactions. One way to do this would be via the inner product of quantile functions expressed in terms of the interactions of corresponding L-moments. Another direction of work is to extend the quantile function based SOFR model to capture possible temporal effects. Finally, normalization of scales across multiple distributional predictors will need to be deeply studied. For example, quantile function $Q_i(p)$ could be normalized within each subject using the transformation $(Q_i(p) - Median_i)/IQR_i$ to make scales more comparable across subjects and variables.

References

- Alzheimer’s Association (2020). 2020 alzheimer’s disease facts and figures. *Alzheimer’s & Dementia* **16**, 391–460.
- Augustin, N. H., Mattocks, C., Faraway, J. J., Greven, S., and Ness, A. R. (2017). Modelling a response as a function of high-frequency count data: The association between physical activity and fat mass. *Statistical methods in medical research* **26**, 2210–2226.
- Bakrania, K., Yates, T., Edwardson, C. L., Bodicoat, D. H., Esliger, D. W., Gill, J. M., Kazi, A., Velayudhan, L., Sinclair, A. J., Sattar, N., et al. (2017). Associations of moderate-to-vigorous-intensity physical activity and body mass index with glycated haemoglobin within the general population: a cross-sectional analysis of the 2008 health survey for england. *BMJ open* **7**, e014456.
- Bigot, J., Gouet, R., Klein, T., Lopez, A., et al. (2018). Upper and lower risk bounds for

- estimating the wasserstein barycenter of random measures on the real line. *Electronic Journal of Statistics* **12**, 2253–2289.
- Dryden, I. L. and Mardia, K. V. (2016). *Statistical shape analysis: with applications in R*, volume 995. John Wiley & Sons.
- Elamir, E. A. and Seheult, A. H. (2003). Trimmed l-moments. *Computational Statistics & Data Analysis* **43**, 299–314.
- Gilchrist, W. (2000). *Statistical modelling with quantile functions*. CRC Press.
- Goldsmith, J., Bobb, J., Crainiceanu, C. M., Caffo, B., and Reich, D. (2011). Penalized functional regression. *Journal of computational and graphical statistics* **20**, 830–851.
- Goldsmith, J., Liu, X., Jacobson, J., and Rundle, A. (2016). New insights into activity patterns in children, found using functional data analyses. *Medicine and science in sports and exercise* **48**, 1723.
- Goldsmith, J., Scheipl, F., Huang, L., Wrobel, J., Gellar, J., Harezlak, J., McLean, M. W., Swihart, B., Xiao, L., Crainiceanu, C., and Reiss, P. T. (2018). *refund: Regression with Functional Data*. R package version 0.1-17.
- Goldsmith, J., Zipunnikov, V., and Schrack, J. (2015). Generalized multilevel function-on-scalar regression and principal component analysis. *Biometrics* **71**, 344–353.
- Haberkamp, M., Moseley, J., Athanasiou, D., de Andres-Trelles, F., Elferink, A., Rosa, M. M., and Magrelli, A. (2019). European regulators’ views on a wearable-derived performance measurement of ambulation for duchenne muscular dystrophy regulatory trials. *Neuromuscular Disorders* **29**, 514–516.
- Hausdorff, J. M., Hillel, I., Shustak, S., Del Din, S., Bekkers, E. M., Pelosin, E., Nieuwhof, F., Rochester, L., and Mirelman, A. (2018). Everyday stepping quantity and quality among older adult fallers with and without mild cognitive impairment: initial evidence for new motor markers of cognitive deficits? *The Journals of Gerontology: Series A* **73**,

1078–1082.

- Hebert, L. E., Weuve, J., Scherr, P. A., and Evans, D. A. (2013). Alzheimer disease in the united states (2010–2050) estimated using the 2010 census. *Neurology* **80**, 1778–1783.
- Hosking, J. R. (1990). L-moments: Analysis and estimation of distributions using linear combinations of order statistics. *Journal of the Royal Statistical Society: Series B (Methodological)* **52**, 105–124.
- Huang, L., Bai, J., Ivanescu, A., Harris, T., Maurer, M., Green, P., and Zipunnikov, V. (2019). Multilevel matrix-variate analysis and its application to accelerometry-measured physical activity in clinical populations. *Journal of the American Statistical Association* **114**, 553–564.
- Ichimura, H. (1991). Semiparametric least squares (sls) and weighted sls estimation of single-index models.
- Irpino, A. and Verde, R. (2013). A metric based approach for the least square regression of multivariate modal symbolic data. In *Statistical models for data analysis*, pages 161–169. Springer.
- Kourtis, L. C., Regele, O. B., Wright, J. M., and Jones, G. B. (2019). Digital biomarkers for alzheimer’s disease: the mobile/wearable devices opportunity. *NPJ digital medicine* **2**, 1–9.
- Lock, E. F., Hoadley, K. A., Marron, J. S., and Nobel, A. B. (2013). Joint and individual variation explained (jive) for integrated analysis of multiple data types. *The annals of applied statistics* **7**, 523.
- Marx, B. D. and Eilers, P. H. (1999). Generalized linear regression on sampled signals and curves: a p-spline approach. *Technometrics* **41**, 1–13.
- Mc Ardle, R., Del Din, S., Galna, B., Thomas, A., and Rochester, L. (2020). Differentiating dementia disease subtypes with gait analysis: feasibility of wearable sensors? *Gait &*

Posture **76**, 372–376.

- McLean, M. W., Hooker, G., Staicu, A.-M., Scheipl, F., and Ruppert, D. (2014). Functional generalized additive models. *Journal of Computational and Graphical Statistics* **23**, 249–269.
- Morris, J. S. (2015). Functional regression. *Annual Review of Statistics and Its Application* **2**, 321–359.
- Morris, J. S., Arroyo, C., Coull, B. A., Ryan, L. M., Herrick, R., and Gortmaker, S. L. (2006). Using wavelet-based functional mixed models to characterize population heterogeneity in accelerometer profiles: a case study. *Journal of the American Statistical Association* **101**, 1352–1364.
- Müller, H.-G. and Yao, F. (2008). Functional additive models. *Journal of the American Statistical Association* **103**, 1534–1544.
- O’Connell, M. J. and Lock, E. F. (2017). *r.jive: Perform JIVE Decomposition for Multi-Source Data*. R package version 2.1.
- Parzen, E. et al. (2004). Quantile probability and statistical data modeling. *Statistical Science* **19**, 652–662.
- Powley, B. W. (2013). *Quantile function methods for decision analysis*. PhD thesis, Stanford University.
- R Core Team (2018). *R: A Language and Environment for Statistical Computing*. R Foundation for Statistical Computing, Vienna, Austria.
- Reider, L., Bai, J., Scharfstein, D. O., Zipunnikov, V., Investigators, M. O. S., et al. (2020). Methods for step count data: Determining “valid” days and quantifying fragmentation of walking bouts. *Gait & Posture* **81**, 205–212.
- Reiss, P. T., Goldsmith, J., Shang, H. L., and Ogden, R. T. (2017). Methods for scalar-on-function regression. *International Statistical Review* **85**, 228–249.

- Shema-Shiratzky, S., Hillel, I., Mirelman, A., Regev, K., Hsieh, K. L., Karni, A., Devos, H., Sosnoff, J. J., and Hausdorff, J. M. (2020). A wearable sensor identifies alterations in community ambulation in multiple sclerosis: contributors to real-world gait quality and physical activity. *Journal of Neurology* pages 1–10.
- Stoker, T. M. (1986). Consistent estimation of scaled coefficients. *Econometrica: Journal of the Econometric Society* pages 1461–1481.
- Takemura, A. (1983). Orthogonal expansion of quantile function and components of the shapiro-francia statistic. Technical report, STANFORD UNIV CA DEPT OF STATISTICS.
- Tibshirani, R. (1996). Regression shrinkage and selection via the lasso. *Journal of the Royal Statistical Society: Series B (Methodological)* **58**, 267–288.
- vanZwet, W. R. (1964). *Convex transformations of random variables*. Mathematisch Centrum, Amsterdam.
- Varma, V. R., Dey, D., Leroux, A., Di, J., Urbanek, J., Xiao, L., and Zipunnikov, V. (2017). Re-evaluating the effect of age on physical activity over the lifespan. *Preventive medicine* **101**, 102–108.
- Varma, V. R., Ghosal, R., Hillel, I., Volfson, D., Weiss, J., Urbanek, J., Hausdorff, J. M., Zipunnikov, V., and Watts, A. (2021). Continuous gait monitoring discriminates community dwelling mild ad from cognitively normal controls. *Alzheimer’s & Dementia: Translational Research & Clinical Interventions* **7**, e12131.
- Varma, V. R. and Watts, A. (2017). Daily physical activity patterns during the early stage of alzheimer’s disease. *Journal of Alzheimer’s Disease* **55**, 659–667.
- Verde, R. and Irpino, A. (2010). Ordinary least squares for histogram data based on wasserstein distance. In *Proceedings of COMPSTAT’2010*, pages 581–588. Springer.
- Wang, L. and Yang, L. (2009). Spline estimation of single-index models. *Statistica Sinica*

pages 765–783.

- Weiss, A., Herman, T., Giladi, N., and Hausdorff, J. M. (2014). Objective assessment of fall risk in parkinson’s disease using a body-fixed sensor worn for 3 days. *PloS one* **9**, e96675.
- Wood, S. N. (2017). *Generalized additive models: an introduction with R*. CRC press.
- Wood, S. N., Pya, N., and Säfken, B. (2016). Smoothing parameter and model selection for general smooth models. *Journal of the American Statistical Association* **111**, 1548–1563.
- Wrobel, J., Zipunnikov, V., Schrack, J., and Goldsmith, J. (2019). Registration for exponential family functional data. *Biometrics* **75**, 48–57.
- Xiao, L., Huang, L., Schrack, J. A., Ferrucci, L., Zipunnikov, V., and Crainiceanu, C. M. (2015). Quantifying the lifetime circadian rhythm of physical activity: a covariate-dependent functional approach. *Biostatistics* **16**, 352–367.
- Yang, H. (2020). Random distributional response model based on spline method. *Journal of Statistical Planning and Inference* **207**, 27–44.
- Yang, H., Baladandayuthapani, V., Rao, A. U., and Morris, J. S. (2020). Quantile function on scalar regression analysis for distributional data. *Journal of the American Statistical Association* **115**, 90–106.
- Yogev-Seligmann, G., Hausdorff, J. M., and Giladi, N. (2008). The role of executive function and attention in gait. *Movement disorders: official journal of the Movement Disorder Society* **23**, 329–342.
- Zhang, Z. and Müller, H.-G. (2011). Functional density synchronization. *Computational Statistics & Data Analysis* **55**, 2234–2249.

Supporting Information

Web Appendix 1-2, Web Tables 1-6 and Web Figures 1-5 referenced in this article are available with supporting information at the Biometrics website on Wiley Online Library.

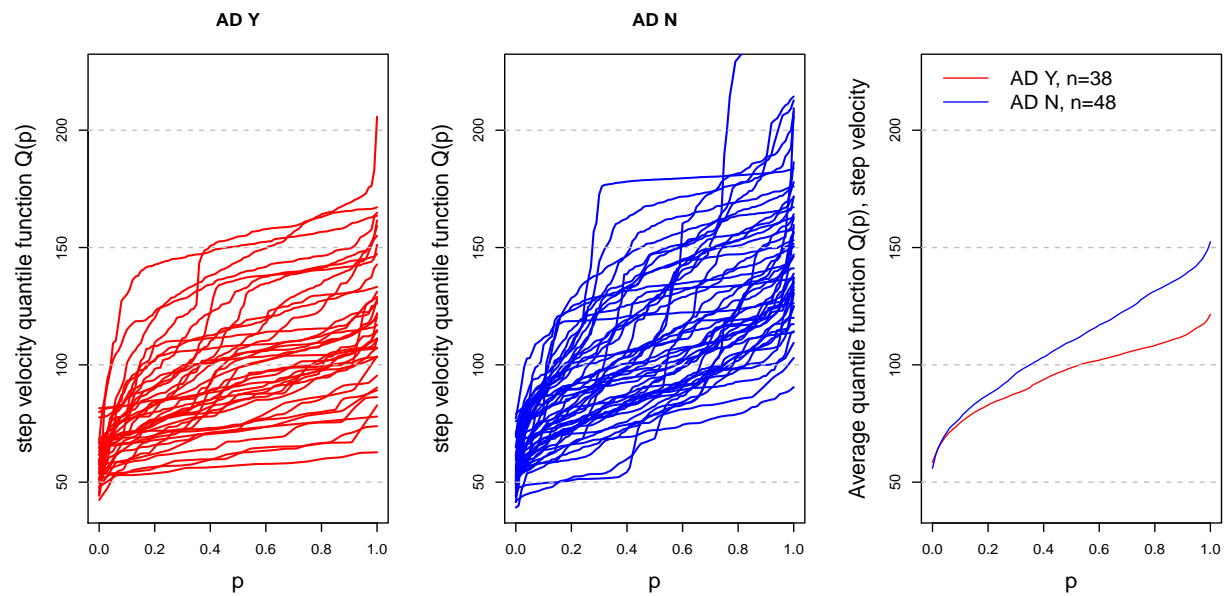


Figure 1: Displayed are the individual (left two panel) and average (right panel) quantile functions of step velocity for AD and controls.

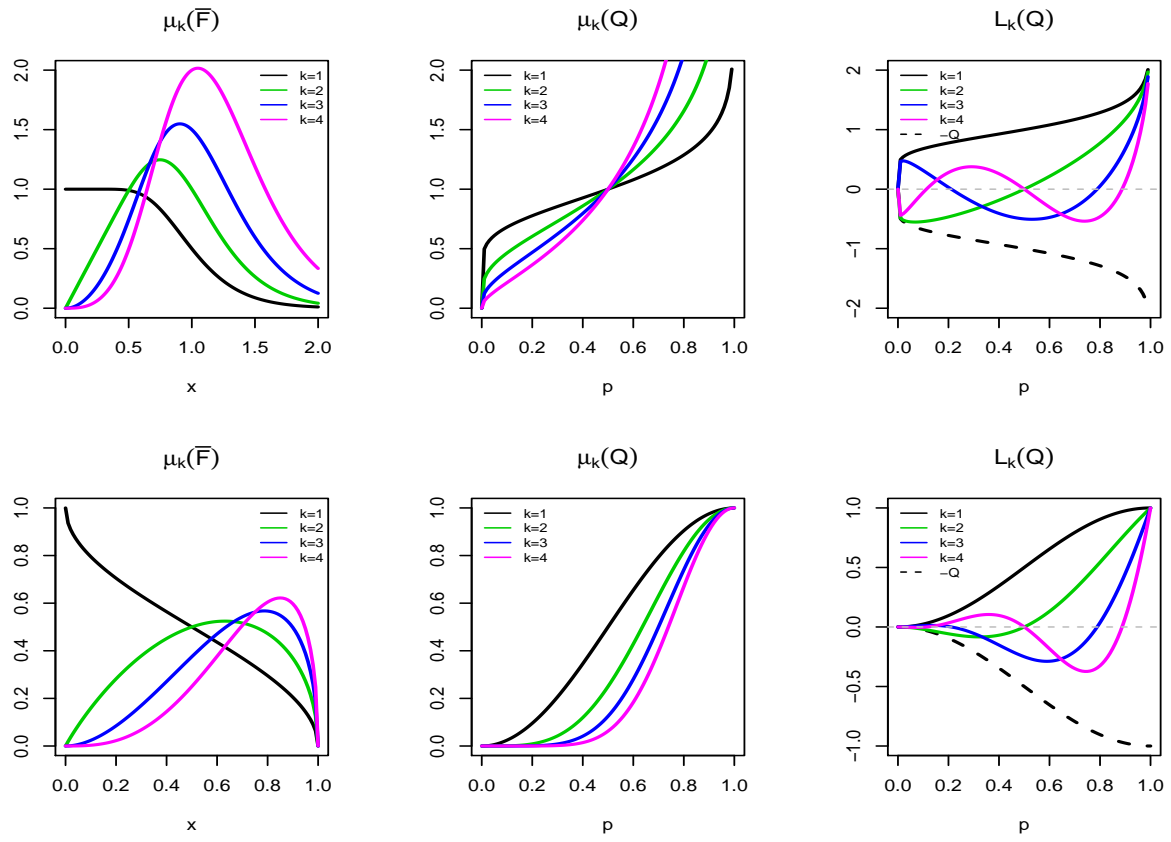


Figure 2: Top: lognormal distribution with $SD = 0.3$. Bottom: beta distribution with $\alpha = \beta = 0.5$.

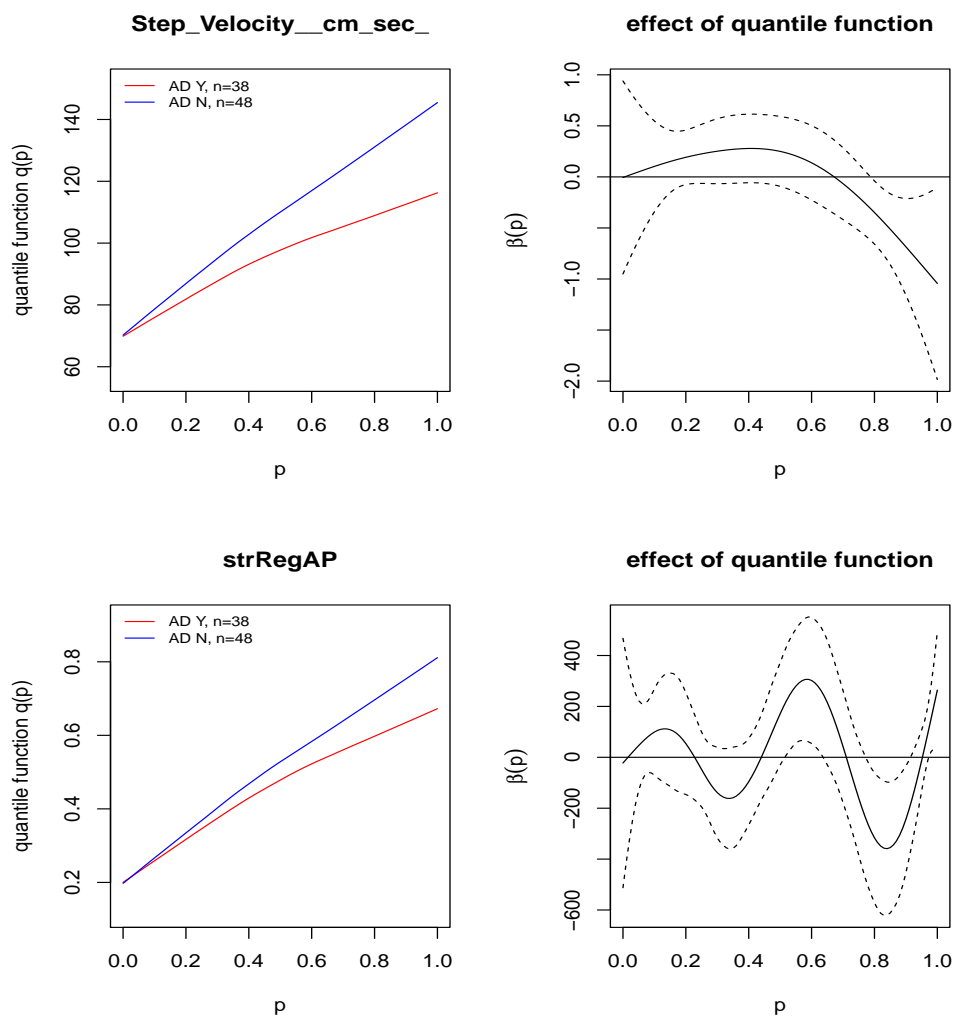


Figure 3: Linear functional effects $\beta(p)$ of quantile functions of `Step_Velocity_cm_sec_` (top) and `strRegAP` (bottom).

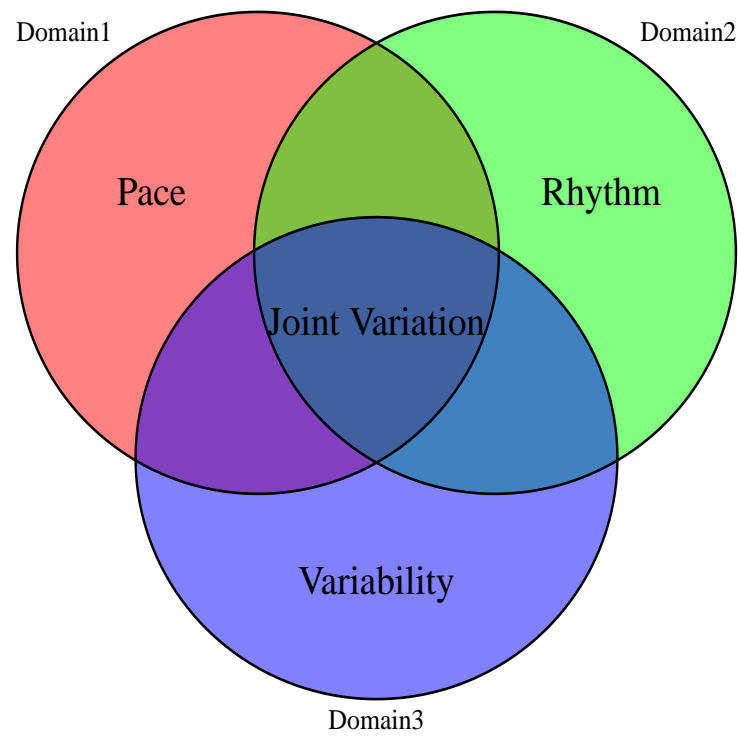


Figure 4: Venn diagram highlighting two main sources of variation: joint (the shaded intersection region) and domain-specific (individual part of each circle).

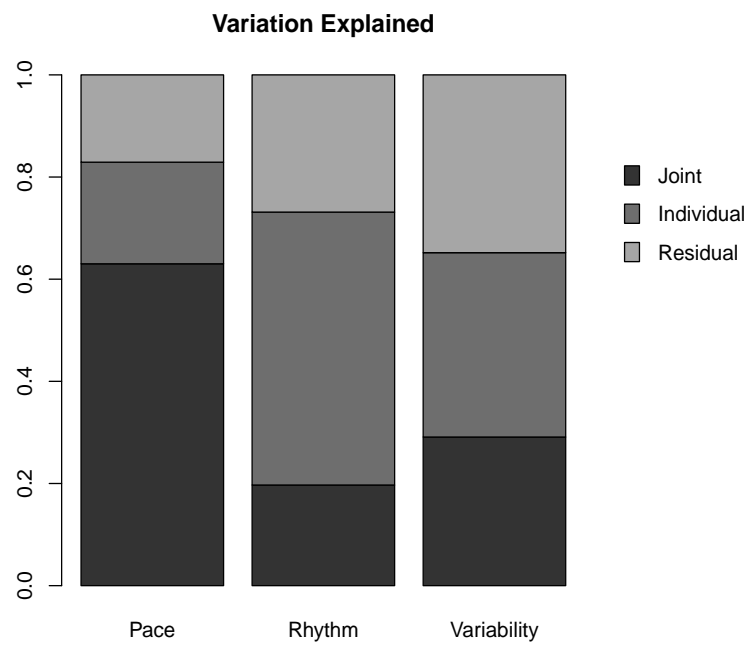


Figure 5: Joint and individual variation explained by each domain from JIVE.

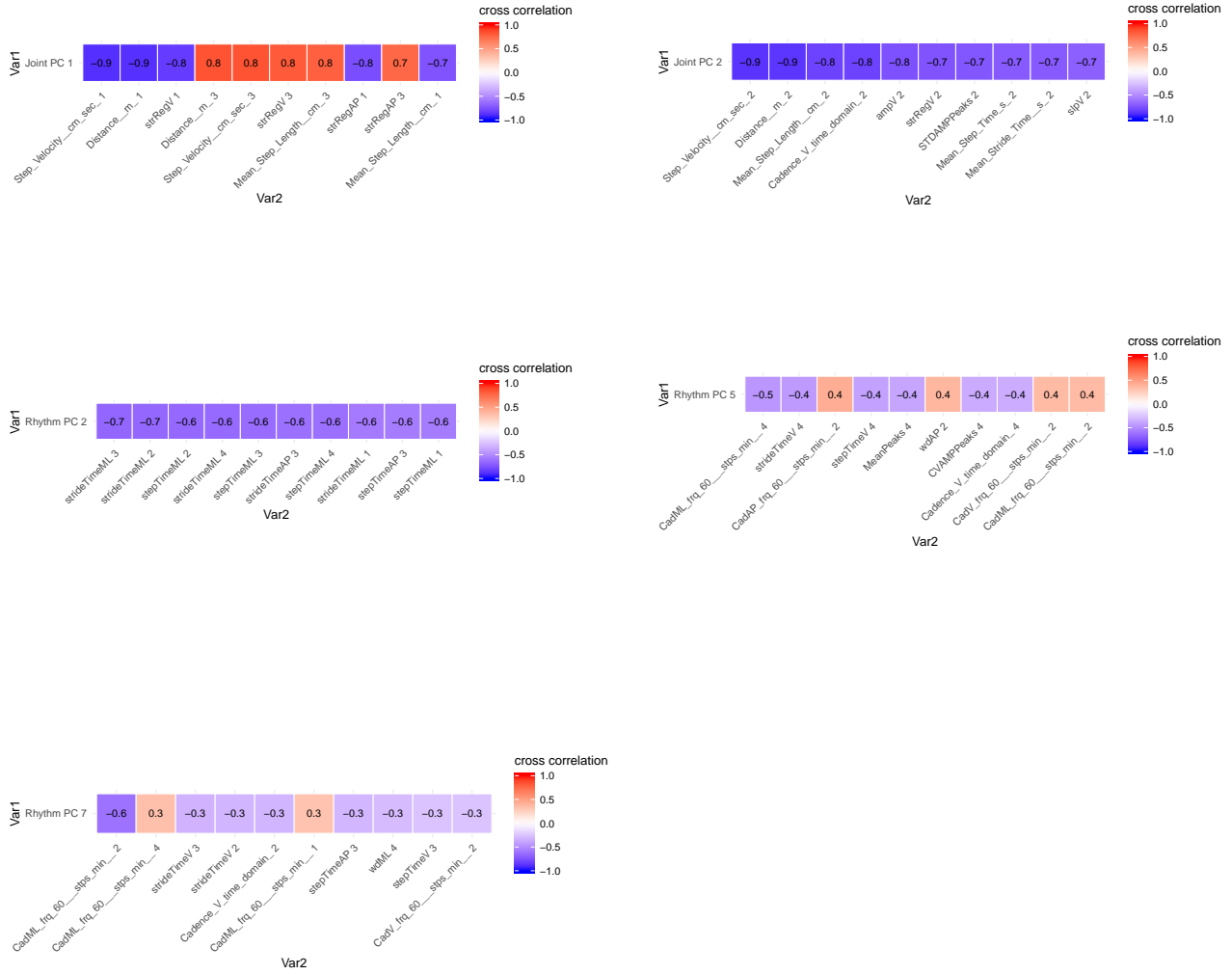


Figure 6: Cross correlation between JIVE PC scores and L-moments. Shown are the top 10 L-moments ranked according to absolute value of correlation with each PC score. “Gait measure r ” represents (r)th L-moment of the particular gait metric.

Table 1: Displayed are the proportion of deviance explained by SOFR and FGAM modelling cognitive status using quantile functions of gait metrics in presence of age and sex. The top 10 metrics have been reported for each of the method.

Variable (ranked for SOFR)	Deviance explained SOFR	Variable (ranked for FGAM)	Deviance explained FGAM
strRegAP	0.58	Mean.Stride.Time._s_	0.63
Step.Velocity._cm._sec_	0.50	Mean.Step.Time.s_	0.63
Distance._m_	0.49	strRegAP	0.59
Cadence.V.time.domain_	0.48	Step.Velocity._cm._sec_	0.50
strideTimeV	0.40	Mean.Step.Length._cm_	0.50
frqML	0.38	frqV	0.50
CV.Step.time	0.38	stepTimeV	0.50
frqV	0.37	strideTimeV	0.50
Mean.Stride.Time._s_	0.37	Distance._m_	0.49
Mean.Step.Time.s_	0.37	Cadence.V.time.domain_	0.48

Table 2: The results of logistic regressions for mild-AD status (adjusted for age and sex) on first four L-moments of strRegAP (Model A1) , Step_Velocity_cm_sec_ (Model A2) and Cadence_V_time_domain_ (Model A3) respectively. Deviance explained using only mean of gait measures (adjusted for age and sex) are provided for comparison in the parenthesis.

Model A1 (strRegAP)			Model A2 (Step Velocity)			Model A3 (Cadence)		
Coef	est	p-value	Coef	est	p-value	Coef	est	p-value
β_0	4.31	0.17327	β_0	18.203	0.00267	β_0	6.338	0.25626
age	-0.044	0.22957	age	-0.151	0.00836	age	-0.048	0.29464
sex (M)	2.113	0.00015	sex (M)	3.706	5.11×10^{-5}	sex (M)	2.740	0.00155
L_1	-0.604	0.85739	L_1	-0.044	0.16441	L_1	0.009	0.84854
L_2	-21.801	0.03457	L_2	-0.480	0.00127	L_2	-1.055	4.2×10^{-5}
L_3	4.621	0.84022	L_3	-0.601	0.03620	L_3	0.002	0.99676
L_4	12.761	0.63239	L_4	-0.212	0.61004	L_4	-0.121	0.90079
Deviance explained	21.58(15.59)%		Deviance explained	48.75(24.20)%		Deviance explained	45.11(17.73)%	

Table 3: The results from linear regression models of cognitive scores (ATTN, VM and EF) on first four L-moments of strRegAP, Step_Velocity_cm_sec_ and Cadence_V_time_domain_, adjusting for age, sex and education. Benchmark models using just age, sex, and education produce adjusted- $R^2_{ATTN} = 0.163$, $R^2_{VM} = 0.2489$, $R^2_{EF} = 0.2754$. Adjusted R-squares using only mean of gait measures (adjusted for age, sex and education) are also provided for comparison in the parenthesis.

Y	Model B1 (strRegAP)			Model B2 (Step Velocity)			Model B3 (Cadence)		
	Coef	est	p-value	Coef	est	p-value	Coef	est	p-value
ATTN	β_0	-2.471	0.017	β_0	-1.964	0.089	β_0	0.738	0.591
	age	0.005	0.640	age	0.007	0.507	age	0.001	0.924
	sex (M)	-0.34	0.031	sex (M)	-0.454	0.006	sex (M)	-0.549	0.002
	edu	0.082	0.001	edu	0.069	0.009	edu	0.074	0.004
	L_1	0.879	0.379	L_1	0.001	0.897	L_1	-0.025	0.035
	L_2	5.879	0.051	L_2	0.039	0.138	L_2	0.124	0.004
	L_3	5.616	0.424	L_3	0.015	0.756	L_3	-0.137	0.122
	L_4	-6.456	0.415	L_4	-0.004	0.961	L_4	0.025	0.882
	adj-Rsq	0.240 (0.172)		adj-Rsq	0.192 (0.173)		adj-Rsq	0.226 (0.154)	
VM	β_0	-4.469	0.036	β_0	-3.283	0.159	β_0	0.655	0.819
	age	0.001	0.973	age	0.009	0.707	age	-0.009	0.666
	sex (M)	-1.296	1×10^{-4}	sex (M)	-1.591	5.8×10^{-6}	sex (M)	-1.583	3.4×10^{-5}
	edu	0.171	0.001	edu	0.119	0.025	edu	0.123	0.022
	L_1	1.173	0.571	L_1	7.4×10^{-6}	0.999	L_1	-0.030	0.213
	L_2	17.118	0.007	L_2	0.131	0.014	L_2	0.315	0.001
	L_3	11.616	0.424	L_3	0.094	0.350	L_3	-0.158	0.389
	L_4	4.214	0.797	L_4	0.119	0.531	L_4	0.215	0.545
	adj-Rsq	0.365 (0.251)		adj-Rsq	0.356 (0.269)		adj-Rsq	0.346 (0.246)	
EF	β_0	-3.307	0.048	β_0	-3.623	0.048	β_0	0.844	0.698
	age	0.004	0.814	age	0.016	0.389	age	-0.002	0.912
	sex (M)	-1.140	2.4×10^{-5}	sex (M)	-1.329	1.5×10^{-6}	sex (M)	-1.368	3.4×10^{-6}
	edu	0.134	0.001	edu	0.108	0.009	edu	0.103	0.012
	L_1	-0.402	0.804	L_1	0.005	0.697	L_1	-0.036	0.053
	L_2	15.992	0.001	L_2	0.087	0.034	L_2	0.294	2.8×10^{-5}
	L_3	-3.396	0.765	L_3	0.051	0.512	L_3	-0.264	0.061
	L_4	-1.960	0.879	L_4	-0.064	0.664	L_4	0.442	0.104
	adj-Rsq	0.377 (0.280)		adj-Rsq	0.376 (0.302)		adj-Rsq	0.397 (0.271)	

**Supporting Information for Distributional data analysis via quantile functions
and its application to modelling digital biomarkers of gait in Alzheimer’s
Disease**

Rahul Ghosal^{1,*}, Vijay R. Varma², Dmitri Volfson³, Inbar Hillel⁴, Jacek Urbanek⁵,

Jeffrey M. Hausdorff^{4,6,7}, Amber Watts⁸ and Vadim Zipunnikov¹

¹ Department of Biostatistics, Johns Hopkins Bloomberg School of Public Health, Baltimore, Maryland USA

² National Institute on Aging (NIA), National Institutes of Health (NIH), Baltimore, Maryland, USA

³Neuroscience Analytics, Computational Biology, Takeda, Cambridge, MA, USA

⁴Center for the Study of Movement, Cognition and Mobility, Neurological Institute,
Tel Aviv Sourasky Medical Center, Tel Aviv, Israel

⁵ Department of Medicine, Johns Hopkins University School of Medicine, Baltimore Maryland, USA

⁶ Department of Physical Therapy, Sackler Faculty of Medicine, and Sagol School of Neuroscience,
Tel Aviv University, Tel Aviv, Israel

⁷Rush Alzheimer’s Disease Center and Department of Orthopedic Surgery,
Rush University Medical Center, Chicago, USA

⁸ Department of Psychology, University of Kansas, Lawrence, KS, USA

**email:* rghosal@ncsu.edu

1. Web Appendix 1: Estimation in Qunatile function based FGAM

For identifiability of the FGAM (model (5) in the paper), the following constraint is imposed: $\sum_{i=1}^n \int_0^1 F(Q_i(p), p) = 0$ (McLean et al., 2014; Wood, 2017). Note that the proposed approach of using $F\{Q(p), p\}$ capturing the smooth effect of the subject-specific quantile function at each quantile level is different from using the transformation approach in McLean et al. (2014), which is focused on studying the smooth diurnal effect $F\{G_t(X(t)), t\}$ using population level distribution function $G_t(x)$. Nevertheless, the same model fitting procedure can be used. In particular, we model the bivariate function $F(\cdot, \cdot)$ using a tensor product of univariate B-spline basis functions. Suppose, $\{B_{Q,k}(q)\}_{k=1}^K$ and $\{B_{P,\ell}(p)\}_{\ell=1}^L$ be a set of known basis functions over q (where $Q(p) = q$) and p , respectively. Then, $F(\cdot, \cdot)$ is modelled using a tensor product two basis functions as $F\{Q_i(p), p\} = \sum_{k=1}^K \sum_{\ell=1}^L \theta_{k,\ell} B_{Q,k}\{Q_i(p)\} B_{P,\ell}(p)$. Using this expansion model (5) (in the paper) can be reformulated as

$$\begin{aligned} g(\mu_i) &= \alpha + \mathbf{Z}_i^T \boldsymbol{\gamma} + \sum_{k=1}^K \sum_{\ell=1}^L \theta_{k,\ell} \int_0^1 B_{Q,k}\{Q_i(p)\} B_{P,\ell}(p) dp \\ &= \alpha + \mathbf{Z}_i^T \boldsymbol{\gamma} + \mathbf{W}_i^T \boldsymbol{\theta}, \end{aligned} \quad (1)$$

where we denote the KL -dimensional vector of $B_{Q,k}\{Q_i(p)\} B_{P,\ell}(p)$'s as \mathbf{W}_i , and $\boldsymbol{\theta}$ is the vector of unknown basis coefficients $\theta_{k,\ell}$'s. Then, the penalized negative log likelihood criterion for estimation is given by

$$S(\psi) = R(\alpha, \boldsymbol{\gamma}, \boldsymbol{\theta}) = -2\log L(\alpha, \boldsymbol{\gamma}, \boldsymbol{\theta}; Y_i, \mathbf{Z}_i, \mathbf{W}_i) + \boldsymbol{\theta}^T \mathbb{P} \boldsymbol{\theta}. \quad (2)$$

Here, $\mathbb{P} = \lambda_q D_q^T D_q \otimes I_K + \lambda_p D_p^T D_p \otimes I_L$ is a penalty matrix consisting of second order row and column penalties imposing smoothness on $F(\cdot, \cdot)$ in both directions (Marx and Eilers, 1998). The parameters are estimated using penalized iteratively re-weighted least squares (P-IRLS) as in McLean et al. (2014). We use the `refund` package (Goldsmith et al., 2018) for implementation of FGAM.

2. Web Appendix 2, JIVE Algorithm using L-moments

Algorithm 1: JIVE using L-Moments of Quantile functions

1. **Goal:** To estimate joint and individual structure in multi-modal distributional data
 2. **Input:** \mathbb{L} , the block data matrix containing L-moments $\mathbf{L}_i^{(d)}$
 3. for $iter = 1$ to A do
 4. Determine ranks s and s_d s.
 5. Estimate \mathbb{J} by rank s SVD of \mathbb{L} , set $\mathbb{J} = \mathbb{U}\mathbb{S}\mathbb{V}^T$
 6. for $d = 1$ to D do
 7. $\tilde{\mathbb{L}}^d = \mathbb{L}^d - \mathbb{J}^d$
 8. Estimate \mathbb{A}^d by rank s_d SVD of $\tilde{\mathbb{L}}^d(\mathbb{I} - \mathbb{V}\mathbb{V}^T)$, set $\mathbb{L}^d = \mathbb{L}^d - \mathbb{A}^d$
 9. Set $\mathbb{L} = \begin{bmatrix} \mathbb{L}^1 \\ \mathbb{L}^2 \\ \vdots \\ \mathbb{L}^D \end{bmatrix}$
 10. **Return** \mathbb{J}, \mathbb{A}^d .
-

3. Supporting Tables

Web Tables 1, 2, 3, 4, 5, 6 referenced in the paper are given below.

[Table 1 about here.]

[Table 2 about here.]

[Table 3 about here.]

[Table 4 about here.]

[Table 5 about here.]

[Table 6 about here.]

4. Supporting Figures

Web Figures 1, 2, 3, 4, 5 referenced in the paper are given below.

[Figure 1 about here.]

[Figure 2 about here.]

[Figure 3 about here.]

[Figure 4 about here.]

[Figure 5 about here.]

References

- Goldsmith, J., Scheipl, F., Huang, L., Wrobel, J., Gellar, J., Harezlak, J., McLean, M. W., Swihart, B., Xiao, L., Crainiceanu, C., and Reiss, P. T. (2018). *refund: Regression with Functional Data*. R package version 0.1-17.
- Marx, B. D. and Eilers, P. H. (1998). Direct generalized additive modeling with penalized likelihood. *Computational Statistics & Data Analysis* **28**, 193–209.
- McLean, M. W., Hooker, G., Staicu, A.-M., Scheipl, F., and Ruppert, D. (2014). Functional generalized additive models. *Journal of Computational and Graphical Statistics* **23**, 249–269.
- Wood, S. N. (2017). *Generalized additive models: an introduction with R*. CRC press.

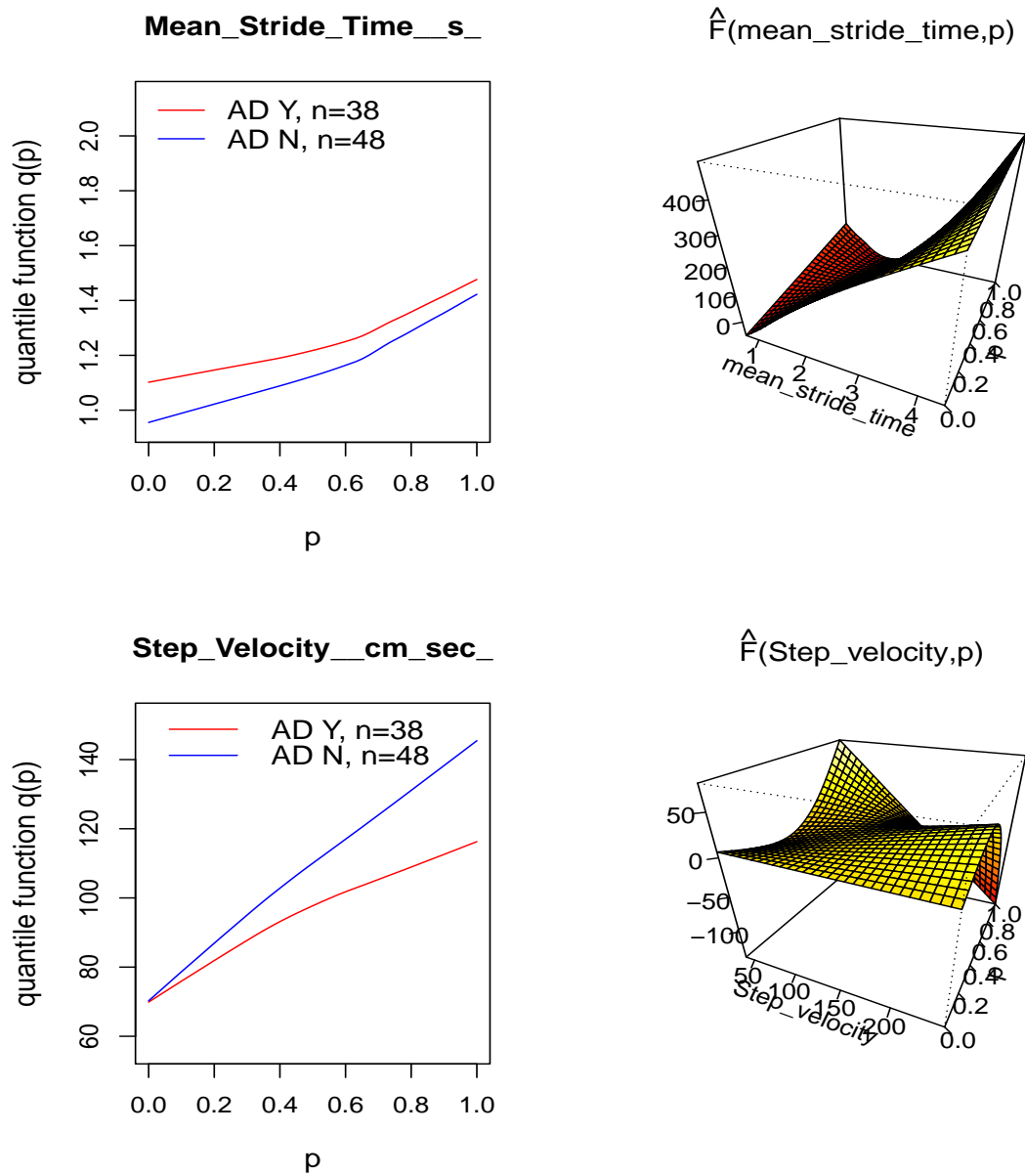


Figure 1: Displayed are additive effects of quantile functions of Mean.Stride.Time.s_ (top) and Step.Velocity.cm.sec_ (bottom) obtained using FGAM and the estimated average quantile functions of two groups (left column) and bivariate surfaces of quantile effect $\hat{F}(q, p)$ (right column).

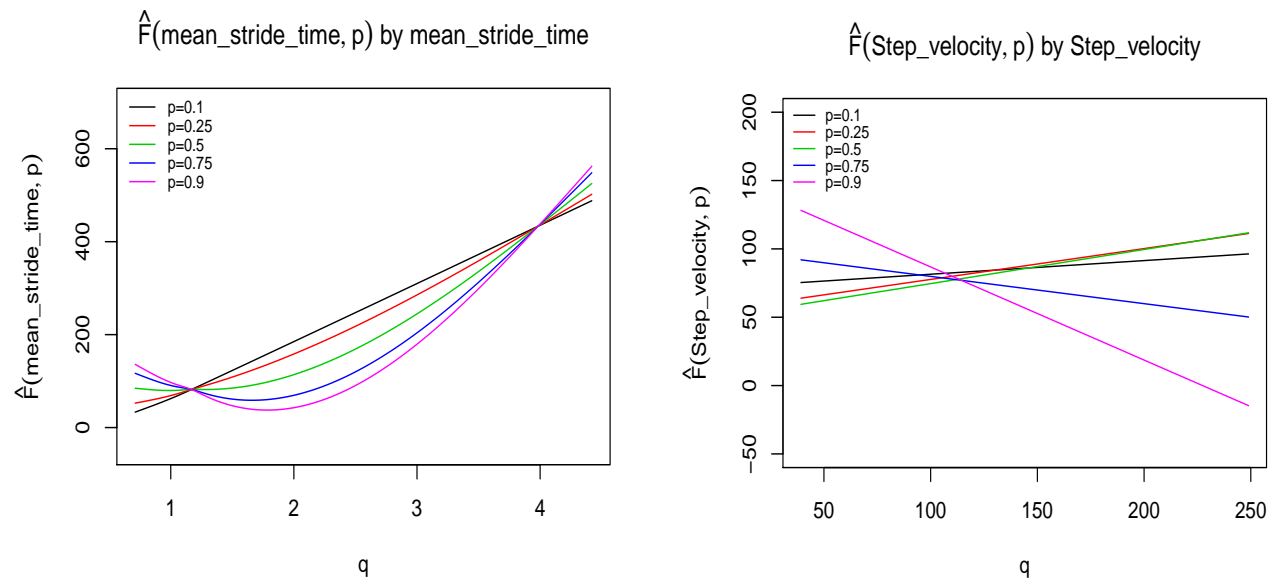


Figure 2: Displayed are sliced effect of the FGAM surface of the two gait metrics $\hat{F}(q, p)$, for $p = 0.1, 0.25, 0.5, 0.75, 0.9$.

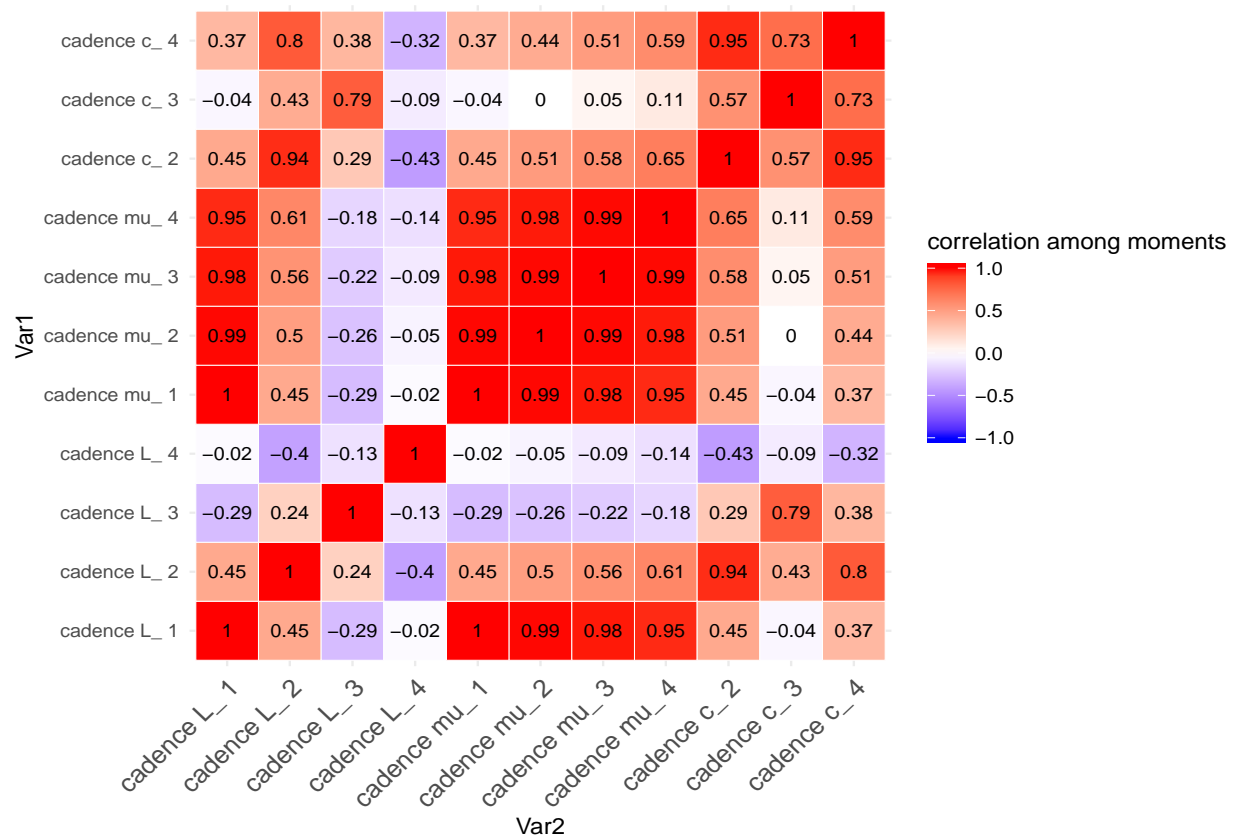


Figure 3: Displayd is the heatmap of sample correlation among the first four L-moment (L) s, regular moments (mu) and central moments (c) of the gait metric Cadence_V_time-domain.

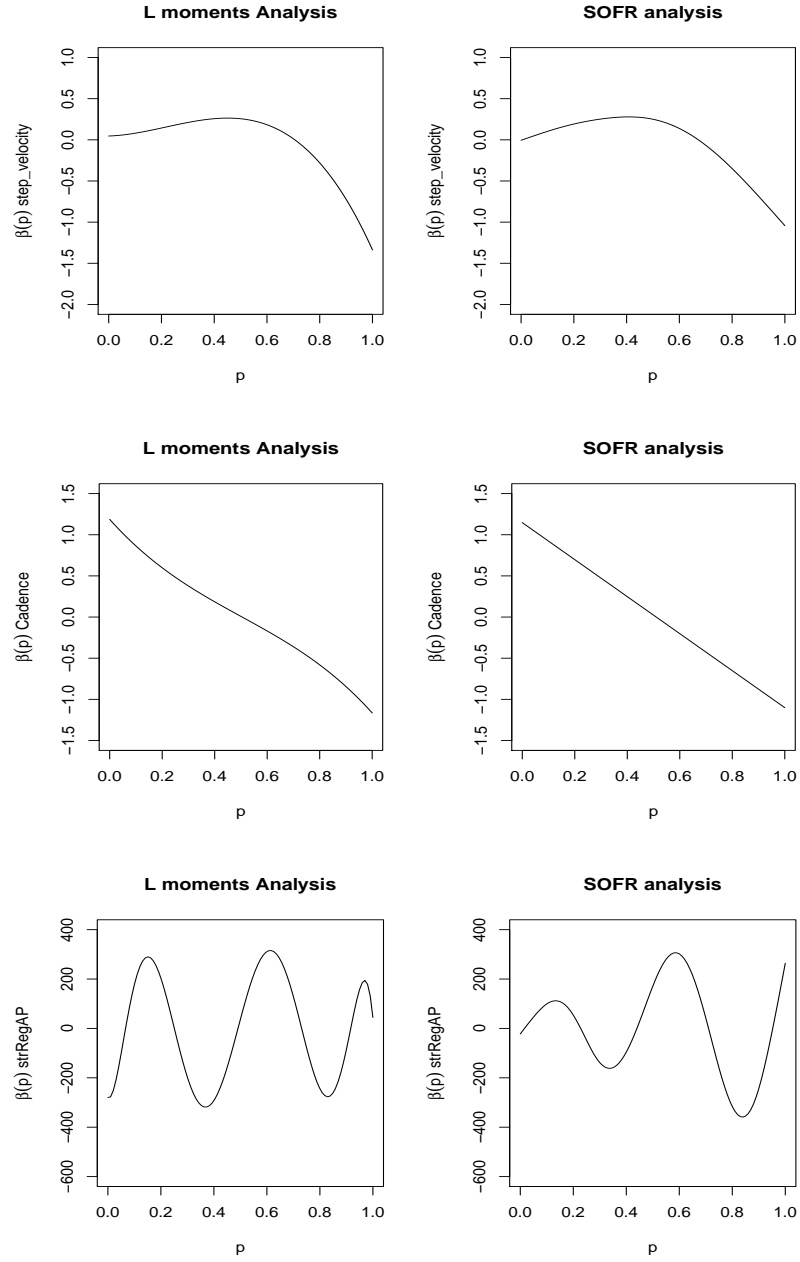


Figure 4: Displayed are linear functional effects $\beta(p)$ from L-moments analysis and SOFR analysis of the gait measures Step_Velocity_cm_sec_ (top), Cadence_V_time_domain_ (middle) and strRegAP (bottom).

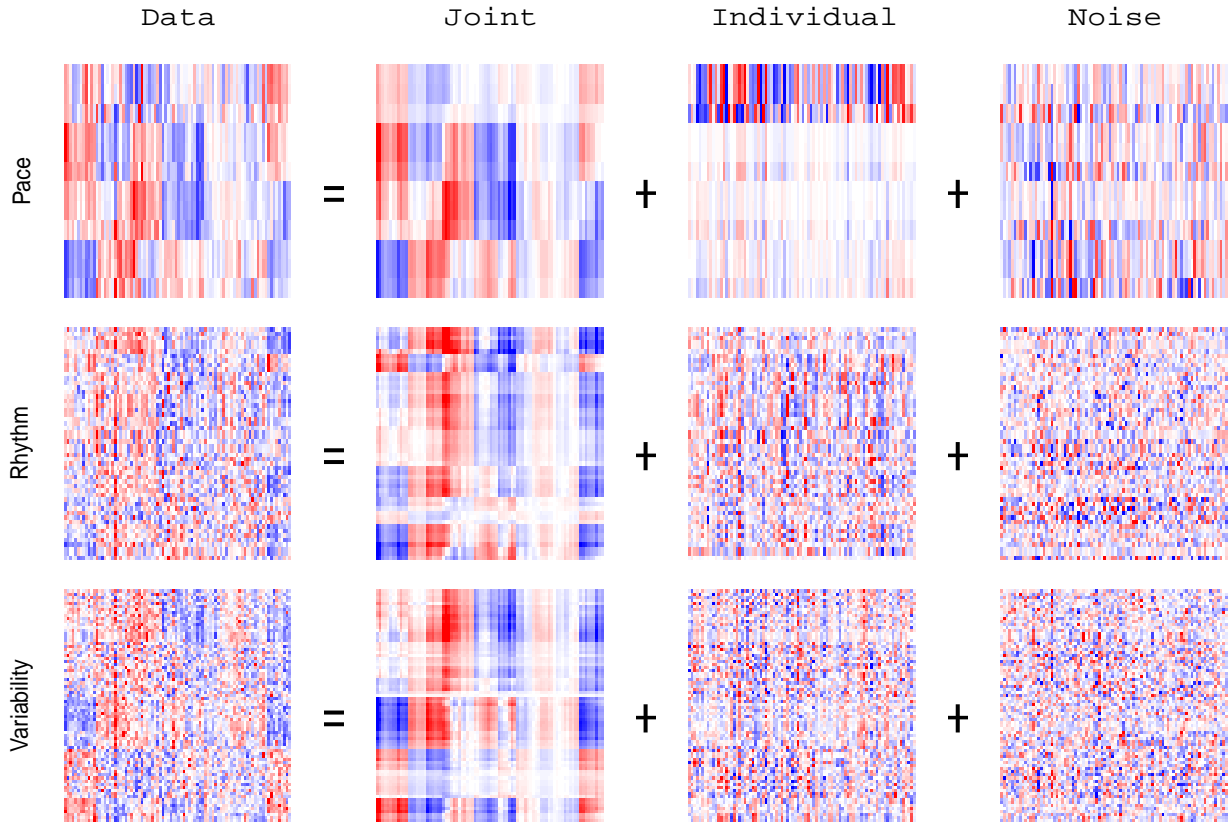


Figure 5: Heatmaps showing JIVE decomposition of the L-moments of gait measures. Columns represent subjects and rows represent features. Rows and columns are ordered by complete linkage clustering of the joint structure.

Table 1: Summary statistics for the complete, AD and CNC samples. No statistical difference between the AD and CNC groups are observed across age, BMI, or VO_2 max. However, AD group had a smaller percentage of females (26.3 vs 68.8 for CNC) and lower education (15.6 years vs 17.4 years for CNC).

Characteristic	Complete sample		AD		CNC		P value
	Mean/Freq	SD	Mean/Freq	SD	Mean/Freq	SD	
Age	73.21	7.13	73.24	7.71	73.19	6.73	0.975
% Female	50	N/A	26.32	N/A	68.75	N/A	<0.001
Years of edu	16.63	3.21	15.59	2.78	17.44	3.31	0.0066
BMI	26.39	6.03	26.38	7.87	26.4	4.13	0.9854
VO2 max	22.06	5.36	21.61	5.24	22.39	5.48	0.5175

Table 2: Displayed are the results from logistic regression models of cognitive status (adjusted for age and sex) on first four regular moments (μ'_r) of strRegAP (Model A11) , Step_Velocity_cm.sec_ (Model A21) and Cadence_V_time.domain_ (Model A31) respectively.

Model A11 (strRegAP)			Model A21 (Step Velocity)			Model A31 (Cadence)		
Coef	est	p-value	Coef	est	p-value	Coef	est	p-value
β_0	-4.098	0.439	β_0	-95.18	0.094	β_0	-713.7	0.202
age	-0.039	0.281	age	-0.058	0.167	age	-0.032	0.373
sex (M)	2.2	7.88×10^{-5}	sex (M)	2.61	1.91×10^{-5}	sex (M)	1.727	0.002
μ'_1	45.79	0.231	μ'_1	4.062	0.075	μ'_1	27.18	0.201
μ'_2	-97.62	0.272	μ'_2	-0.059	0.0712	μ'_2	-0.381	0.203
μ'_3	66.44	0.352	μ'_3	3.61×10^{-4}	0.069	μ'_3	0.002	0.206
μ'_4	-10.35	0.450	μ'_4	-7.9×10^{-7}	0.067	μ'_4	-5.28×10^{-6}	0.210
Deviance explained		21.01%	Deviance explained		30.29%	Deviance explained		20.27%

Table 3: Displayed are the results from logistic regression models of cognitive status (adjusted for age and sex) on mean and three central moments (μ_2, μ_3, μ_4) of strRegAP (Model A12), Step_Velocity_cm.sec_ (Model A22) and Cadence_V_time.domain_ (Model A32) respectively.

Model A12 (strRegAP)			Model A22 (Step Velocity)			Model A32 (Cadence)		
Coef	est	p-value	Coef	est	p-value	Coef	est	p-value
β_0	4.735	0.158	β_0	15.58	0.011	β_0	3.302	0.610
age	-0.056	0.155	age	-0.015	0.012	age	-0.051	0.295
sex (M)	2.405	6.03×10^{-5}	sex (M)	4.01	4.79×10^{-5}	sex (M)	2.898	0.001
μ_1'	-1.097	0.692	μ_1'	-0.036	0.168	μ_1'	0.020	0.696
μ_2	-65.056	0.003	μ_2	-0.009	0.024	μ_2	-0.045	0.003
μ_3	-45.54	0.515	μ_3	-1.52×10^{-4}	0.141	μ_3	-3×10^{-4}	0.595
μ_4	46.60	0.2438	μ_4	1.1×10^{-7}	0.949	μ_4	1.66×10^{-5}	0.484
Deviance explained		28.1%	Deviance explained		48.14%	Deviance explained		47.15%

Table 4: Complete list of the gait measures, their descriptions and associated domains.

Gait Measure	Description	Domain	Gait Measure	Description	Domain
Activity Level [g]	mean signal vector magnitude	Amplitude	Cadence V (time domain) [steps/min]	number of steps per minute	Rhythm
mg V,ML,AP [g]	acceleration range	Amplitude	rms V,ML,AP [g]	acceleration root mean square	Amplitude
frq V,ML,AP [Hz]	dominant frequency of power spectrum	Rhythm	amp V,ML,AP [g2/Hz]	amplitude of the dominant frequency	Variability
wd V,ML,AP [Hz]	width of the dominant frequency	Variability	slp V,ML,AP [g2/Hz2]	amp/wd	Variability
stpReg V,ML,AP [unitless]	step regularity	Symmetry	strReg V,ML,AP [unitless]	stride regularity	Variability
stepSym V,ML,AP [unitless]	step symmetry (=stpReg/strReg)	Symmetry	stepTime V,ML,AP [s]	step time (calculated from autocorrelation function)	Rhythm
strideTime V,ML,AP [s]	stride time (calculated from autocorrelation function)	Rhythm	HR v,ml,ap [unitless]	harmonic ratio	Symmetry
Cad V,ML,AP(frequency domain) [steps/min]	frq *60	Rhythm	Mean Stride Time [s]	mean stride time	Rhythm
CV Stride Time [%]	100*(standard Deviation/mean)	Variability	Mean Step Time[s]	mean step time	Rhythm
CV Step time [%]	100*(standard Deviation/mean)	Variability	Mean Step Length [cm]	mean step length	Pace
CV Step-length	100*(standard Deviation/mean)	Variability	Step Velocity [cm/sec]	mean step length/mean step time	Pace
Distance [m]	sum of step length	Pace	MeanPeaks	mean of peaks	Rhythm
STDPeaks	sd of peaks	Variability	CVPeaks	CV of peaks	Variability
MeanAMPPeaks	mean peak amplitudes (time domain)	Amplitude	STDAAMPeaks	sd of peak amplitudes (time domain)	Variability
CVAMPPeaks	100*(standard Deviation/mean)	Variability			

Table 5: Displayed are the results from generalized additive models (GAM) of cognitive scores (ATTN, VM and EF) on first four L-moments of strRegAP , Step_Velocity_cm.sec_ and Cadence_V_time_domain_ after adjusting for age, sex and education. Benchmark models using age, sex and education produce (adjusted) $R^2_{ATTN} = 0.163$, $R^2_{VM} = 0.2489$, $R^2_{EF} = 0.2754$. A significant improvement (around 17% – 38% gain) is noticed in terms of adjusted R-squared compared to models B1-B3 (Table 3 in the paper) indicating potential non-linearity in the effects of the subject-specific L-moments.

Y	Model B1 (strRegAP)		Model B2 (Step Velocity)		Model B3 (Cadence)	
	Coef	p-value	Coef	p-value	Coef	p-value
ATTN	β_0	0.006	β_0	0.067	β_0	0.217
	age	0.049	age	0.340	age	0.831
	sex (M)	0.022	sex (M)	0.009	sex (M)	0.007
	edu	0.004	edu	0.005	edu	0.003
	$h_1(L_1)$	0.024	$h_1(L_1)$	0.876	$h_1(L_1)$	0.092
	$h_2(L_2)$	0.002	$h_2(L_2)$	0.0471	$h_2(L_2)$	0.005
	$h_3(L_3)$	0.179	$h_3(L_3)$	0.482	$h_3(L_3)$	0.422
	$h_4(L_4)$	0.177	$h_4(L_4)$	0.636	$h_4(L_4)$	0.874
	adj-Rsq	0.395	adj-Rsq	0.232	adj-Rsq	0.259
VM	β_0	0.173	β_0	0.159	β_0	0.614
	age	0.687	age	0.435	age	0.740
	sex (M)	0.00057	sex (M)	1.6×10^{-5}	sex (M)	0.00026
	edu	0.00344	edu	0.0126	edu	0.011
	$h_1(L_1)$	0.265	$h_1(L_1)$	0.444	$h_1(L_1)$	0.678
	$h_2(L_2)$	2.59×10^{-5}	$h_2(L_2)$	0.00875	$h_2(L_2)$	3.29×10^{-5}
	$h_3(L_3)$	0.071	$h_3(L_3)$	0.170	$h_3(L_3)$	0.748
	$h_4(L_4)$	0.0149	$h_4(L_4)$	0.567	$h_4(L_4)$	0.715
	adj-Rsq	0.472	adj-Rsq	0.435	adj-Rsq	0.444
EF	β_0	0.064	β_0	0.079	β_0	0.293
	age	0.337	age	0.261	age	0.826
	sex (M)	0.00012	sex (M)	2.8×10^{-6}	sex (M)	9.04×10^{-5}
	edu	0.00226	edu	0.007	edu	0.005
	$h_1(L_1)$	0.273	$h_1(L_1)$	0.252	$h_1(L_1)$	0.138
	$h_2(L_2)$	0.00051	$h_2(L_2)$	0.0164	$h_2(L_2)$	0.00013
	$h_3(L_3)$	0.474	$h_3(L_3)$	0.866	$h_3(L_3)$	0.163
	$h_4(L_4)$	0.413	$h_4(L_4)$	0.916	$h_4(L_4)$	0.058
	adj-Rsq	0.491	adj-Rsq	0.407	adj-Rsq	0.455

Table 6: Results from logistic regression of cognitive status on JIVE scores, adjusting for age and sex.

Predictor	Beta	p-value	Predictor	Beta	p-value
age	-0.06167	0.453812	Rhythm-PC2	-0.86731	0.045292
sex	6.13591	0.000378	Rhythm-PC5	-1.87063	0.014383
joint-PC1	1.05257	0.044063	Rhythm-PC7	1.65990	0.006741
joint-PC2	2.93640	0.000728	Variability-PC4	-0.43651	0.441194
Pace-PC1	0.82707	0.214616	Variability-PC7	0.35954	0.418637
Pace-PC2	1.41231	0.070124	Variability-PC9	-0.69622	0.182581
Rhythm-PC1	0.45852	0.347566			